2015

Tipping the Balance of Double-Strand Break Repair in Cells Modeling Hutchinson-Gilford Progeria Syndrome

Andrew Robert Patrick
University of South Carolina

Tipping the Balance of Double-Strand Break Repair in Cells Modeling Hutchinson-Gilford Progeria Syndrome

by

Andrew Robert Patrick

Bachelor of Science
The Ohio State University, 2009

Submitted in Partial Fulfillment of the Requirements

For the Degree of Master of Science in

Biological Sciences

College of Arts and Sciences

University of South Carolina

2015

Accepted by:

Alan Waldman, Director of Thesis

Deanna Smith, Reader

Austin Hughes, Reader

Lacy Ford, Senior Vice Provost and Dean of Graduate Studies

Dedication

This thesis is dedicated first to St. Jude the Apostle, Help of the Hopeless, and second to St. Thomas Aquinas, the Angelic Doctor, and finally, to the Blessed Virgin, ora pro nobis peccatoribus nunc et in hora mortis nostrae.

Acknowledgements

The author would like to thank Dr. Alan Waldman for his direction as mentor of an unworthy protégé. The author is also indebted to Dr. Barbara Waldman, Yibin Wang, Shen Li, Sona Chowdhary, and Lauren Vaughn for assistance in the laboratory and to the other members of the committee, Dr. Deanna Smith and Dr. Austin Hughes. Finally, the author acknowledges Edward and Jeanette Patrick for their previous contributions to meiotic recombination, without which this work would not be possible.

Abstract

Hutchinson-Gilford Progeria Syndrome is disease of highly accelerated aging. In addition to appearing physically old mere months after birth, patients suffer from maladies typical of the elderly, including heart attack and stroke, two factors which contribute to an average life expectancy of 14 years. The source of progeria has been identified as progerin, a defective variant of nuclear lamina protein lamin A. Progerin has also been found natively in healthy cells (concentration increasing with age), and is known to adversely affect nuclear morphology and chromosomal integrity. This thesis sought to investigate the effect of progerin upon which pathways were favored in the repair of DNA double-strand breaks. Plasmids were engineered for use in the creation of cell lines inducible for progerin expression. In addition, immortalized human fibroblast cells were transfected to express progerin constitutively. These cells were assayed for the relative rates of different modes of repair after spontaneous and double-strand break-induced recombination. It was discovered that the progerin-expressing cells repair damage via non-homologous end joining at a higher rate than control cells, though there are significant caveats to these data.

Table of Contents

List of Tables

List of Figures

List of Abbreviations

CO.....crossover

DSB.....double-strand break

GC.....gene conversion

HDD.....homology dependent deletion

HGPS..... Hutchinson-Gilford progeria syndrome

LOH.....loss of heterozygosity

NHEJ..... non-homologous end joining

SDSA..... synthesis dependent strand annealing

SSA..... single strand annealing

Chapter 1: Introduction

DNA Double Strand Break Repair

DNA Double-strand breaks (DSB) pose one of the more urgent threats to cell viability. Such breaks may be caused by ionizing radiation, reactive oxygen species, or stalled replication forks (O'Driscoll and Jeggo 2006, Sonoda et al. 2006). A break that is not identified quickly risks being "repaired" by joining it to an unrelated fragment from elsewhere in the genome. The consequences of such genome instability are severe and unpredictable; one of the few that is well characterized is the Philadelphia Chromosome, a translocation which creates a fusion oncogene (Collins et al. 1987, Somervaille and Cleary 2010). Dividing cells that fail to repair the break destroy a large segment of the genome upon mitosis since one side of the break is not attached to a centromere. The other fragment is immediately vulnerable to erosion for lacking a telomere, and it poses a threat of translocation to any subsequent DSB repair events, increasing the likelihood of further errors. Ultimately, unresolved DSBs are nearly universally fatal (McVey and Lee 2008).

The damage site of a DSB activates a signal-transduction pathway through phosphatidylinositol 3-kinase related kinases (PIKK) (Jackson 2002). Two that are known are ataxia telangiectasia mutaed (ATM) and ataxia telangiectasia and RAD3-related (ATR). The ATM pathway is linked to H2A histone family member X (H2AFX), tumor protein 53 binding protein 1 (TP53BP1), and breast cancer 1 early onset (BRCA1) (Stiff et al. 2004); ATM itself regulates cell cycle arrest at the G1-S checkpoint (by way of p53 and p21) and at the G2-M checkpoint (Lukas et al. 2004).

When a DSB is found (Fig 1.1 A), it may be repaired by the process called homologous recombination (HR). Both sides of the break site are resected to produce 3' overhangs (Fig 1.1 B). In humans, the exposed single strands are bound by multiple units RAD51 in a helical structure apparently conserved from bacteria (Ogawa et al. 1993). In one of the known variations of HR, one strand is guided by this complex to a homologous location, the "donor," which is usually the same locus on the sister chromatid or the homologous chromosome, though more complex substrates are possible (Wang et al 2011). The RAD51-DNA complex unwinds the donor site to initiate strand invasion and allow the overhang to base pair (Fig 1.1 C, Baumann and West 1998). Likewise, the other exposed 3' overhang pairs complementarily to the other strand of the donor (Fig 1.1 D). The intact donor then serves as a template for a DNA polymerase to

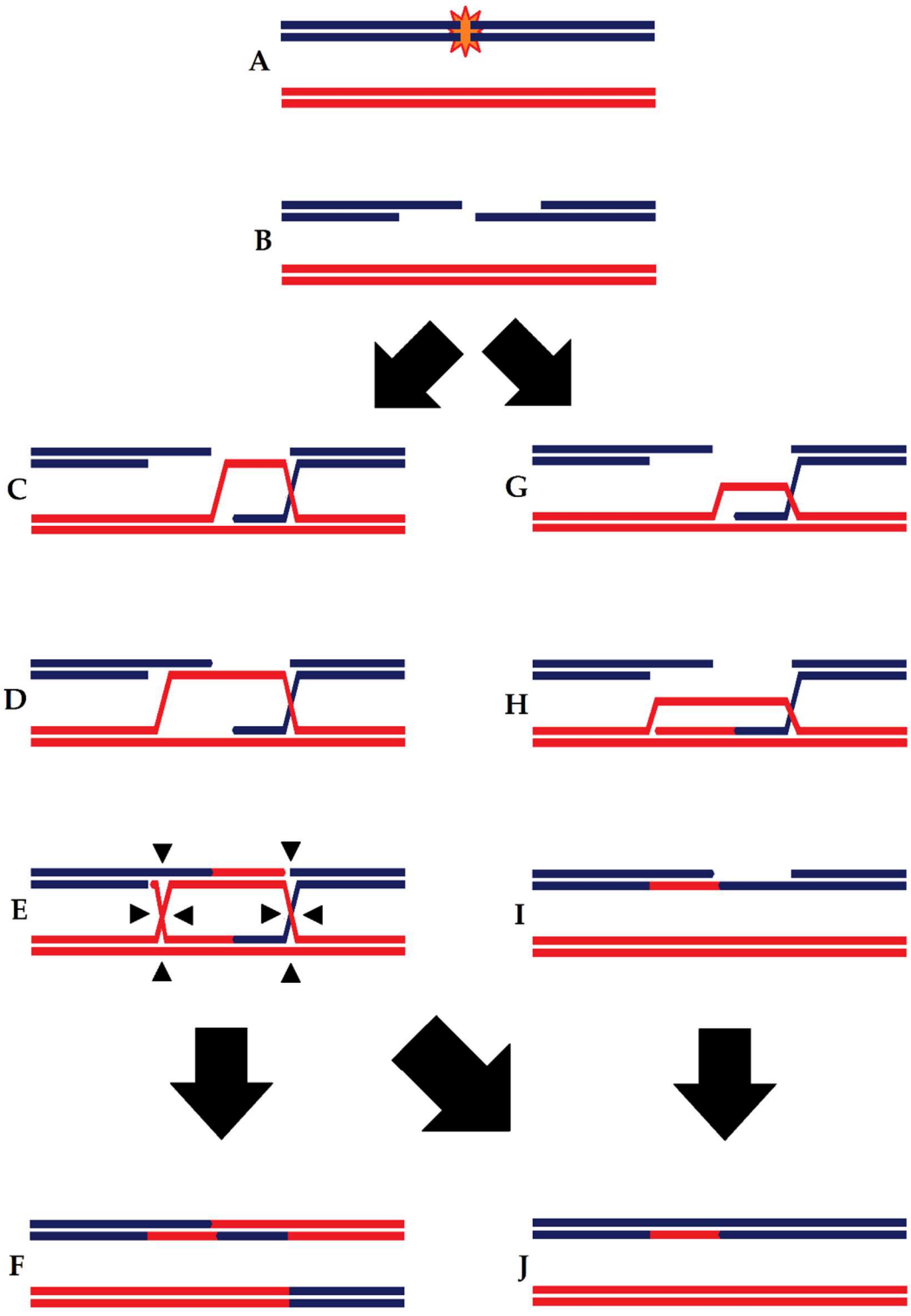

Figure 1.1 Homologous Recombination

See text for details.

replace the resected bases (Fig 1.1 E). Each of the invasion sites consists of a four-stranded, cross-shaped DNA structure called a Holliday Junction. A junction is capable of migrating and may thereby expand the repair site beyond the initial region of damage and resection, resulting in stretches of paired bases derived from different chromosomes. The complex of repair proteins must finally resolve the double Holliday Junctions by cleavage and ligation. These cleavages are directional and result in either crossover (CO, Fig 1.1 F) or non-crossover (also called gene conversion (GC, Fig 1.1 J)) events. Crossovers, specifically, exchange all genetic material on the distal side of the break between the two chromosomes or chromatids. Because HR is active from late S phase through G2, crossover between two chromosomes may result in four unique chromatids rather than the expected two pairs of identical sisters (Fig 1.2). When these non-identical chromatids segregated upon mitosis, there is a roughly 50% chance that the daughter cells will receive two alleles derived from the same chromosome, a phenomenon called loss of heterozygosity (LOH). Loss of heterozygosity is implicated in cancer as an explanation for the apparent failure of what should be the functioning dominant alleles of tumor-suppressor genes: the alleles are still functional, but they were not inherited by the pre-cancerous cell. This correlation is firmly established, so much so that the coincidence of cancer and loss of heterozygosity is taken as evidence that the affected gene is a

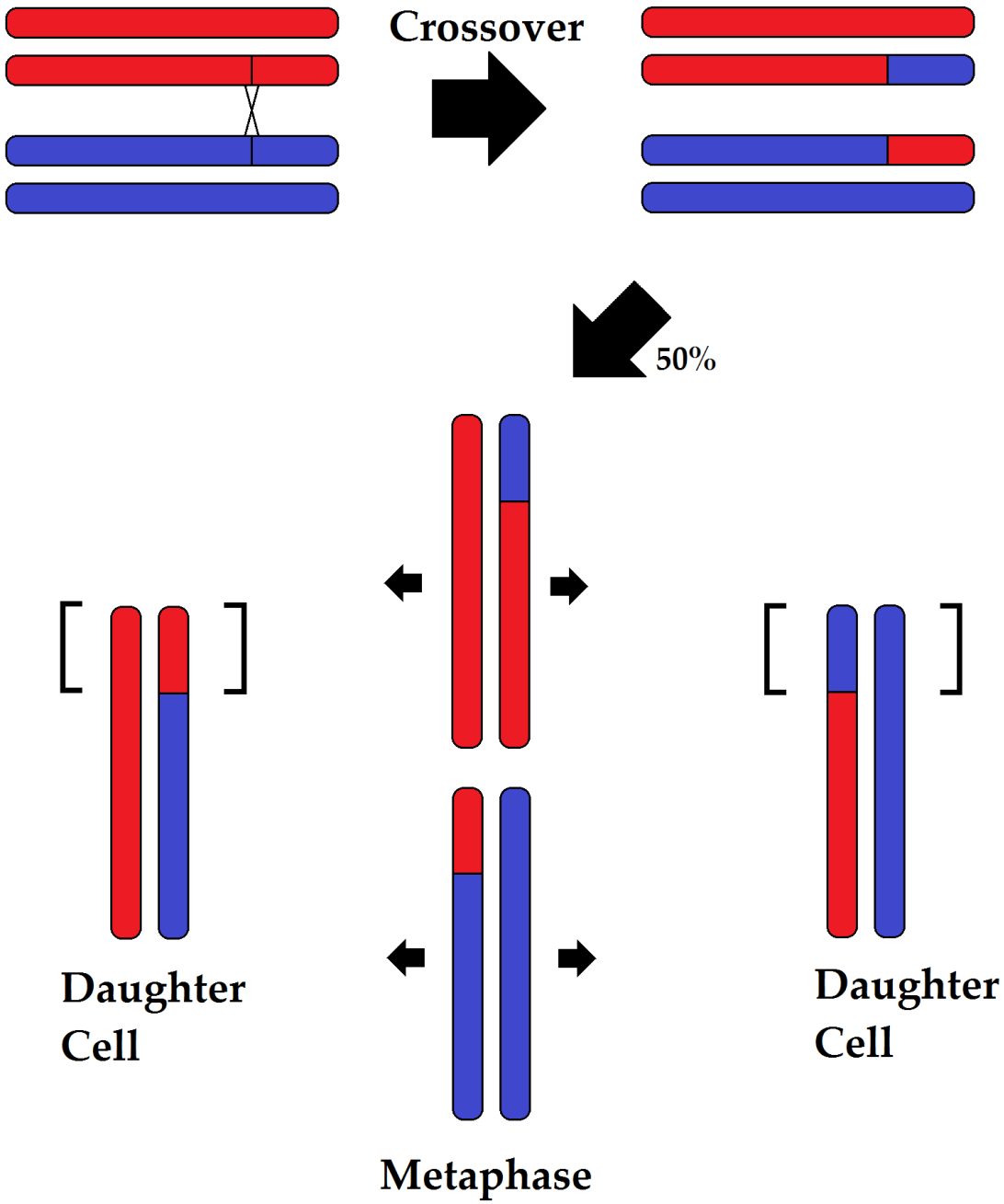

Figure 1.2 Loss of Heterozygosity

Following a single crossover, the subsequent mitosis has a 50% chance of leaving each daughter cell with two haplotypes derived from the same chromosome, as shown by the brackets.

tumor suppressor. Excepting probability, there is nothing to prevent multiple crossover events from occurring to the same chromosome, meaning the chromosome can resolve as a patchwork of alleles originating from both itself and its homologue.

In an alternate pathway, the repair event may also progress without a second strand invasion (Fig 1.1 G). After synthesis extends the 3' overhang (Fig 1.1 H), branch migration may permit the invading strand to detach from the homologous chromosome and anneal to its original complement strand (Fig 1.1 I). The remaining gap is then closed via synthesis and ligation (Fig 1.1 J). This pathway is termed Synthesis Dependent Strand Annealing (SDSA) and cannot result in crossover.

It has been suggested (O'Driscoll and Jeggo 2005) that the primary function of HR is to resolve DSBs that arise due to stalled replication forks (Cha and Kleckner 2002); this is supported by the observation that HR deficient cells are not particularly vulnerable to radiation yet highly vulnerable to crosslinking (O'Driscoll and Jeggo 2005, Thompson and Schild 2001).

Alternatively, a break site may be repaired through Non-Homologous End Joining (NHEJ) wherein the two sides of the break are rejoined by complexes of proteins which assemble on either side of the break. The KU heterodimer first binds the break site and recruits DNA-dependent protein kinase (DNA-PKcs),

DNA polymerase μ or λ, and a ligase (McVey and Lee 2008). The damage which caused the break site does not necessarily leave behind complementary single-stranded ends, so the repair complex may resect the break site to reveal homology. This process is imprecise and may result in deletions in excess of 1 kbp (Wang et al. 2011).

In the certain circumstances, such as a defect in one of the constituent proteins of non-homologous end joining, the two ends are resected in search of microhomology (homology of only a few bases) in a process called Microhomology-Mediated End Joining (MMEJ) (McVey and Lee 2008). Microhomology mediated end joining is necessarily error-prone due to the required loss of bases, and its lax homology requirement renders it prone to join unrelated sequences.

If resection reveals long regions of homology, RAD52 may initiate single strand annealing (SSA). The two overhangs are made to base pair at the repeats with no consideration for sequences 3' to those repeats, forcing unpaired bases to hang loosely away from the repair site. These sequences are digested by an endonuclease before the break is finally sealed by ligation, leading to significant deletions in the wake of a single-strand annealing repair event. (McVey and Lee 2008).

Unlike HR, NHEJ and its related mechanisms are active throughout the cell cycle and, therefore, cover more instances of damage. It may be interpreted that HR is the most favorable, but not always feasible, method to repair DSBs, and NHEJ, MMEJ, and SSA are more urgent means to remedy a critical problem. Regardless of how unfaithful the repair is, it is almost certainly less destructive than neglecting to repair a DSB altogether.

Aging as a Disease of DSB Repair

The issue of repair in general and DSB in particular becomes more pronounced as the organism advances in age. In addition to an accumulating load of mutations (Morley 1998), mutations also occur at a greater rate in aged individuals (Stuart and Glickman 2000). This is not necessarily a positive-feedback mechanism, but perhaps the result of a separate element of the biology of aging (Gorbunova and Seluanov 2005).

Studies of transgenic mice have revealed that advanced age is associated with large and diverse genome rearrangements (Dolle et al. 1997, as cited in Gorbunova and Seluanov 2005). These events were not observed to have occurred at homologous locations, meaning NHEJ, rather than HR, was used in their repair. The coincidence of age and error-prone DSB repair suggests greater errors during non-homologous end joining and/or increased reliance upon same (relative to HR) as the organism ages. DSBs themselves are implicated as a signal

that induces senescence (Gorbunova and Seluanov, 2005), illuminating further the network of effects and causes. Indeed, disruption of various DSB repair factors, including KU and DNA-PKcs, accelerate senescence of cells in culture and cause organisms to develop sundry side-effects usually associated with aging, such as osteoporosis, atherosclerosis, alopecia, and achromotrichia (Gorbunova and Selunov 2005).

Similar phenomena have been observed in human genetic disorders. First described in 1886 by Jonathan Hutchinson, Hutchinson-Gilford Progeria Syndrome (HGPS) is a genetic disorder characterized by patients developing symptoms resembling old age as young children. Within the first year after birth, patients develop alopecia, reduced growth, cardiovascular disease, macrocephaly, and other symptoms, culminating in a life expectancy of approximately 14 years (Ackerman and Gilbert-Barness 2002, Doming Domínguez-Gerpe and Araújo-Vilar 2008); death commonly results from heart attack or stroke (Baker, Baba, and Boesel 1981, as cited in Cao et al. 2006). Due to the early mortality, the disorder is rarely inherited and usually arises from a *de novo* mutation in LMNA, the gene for nuclear lamina protein lamin A. Lamin A is a filamentous protein which polymerizes as part of the nuclear lamina during interphase (Broers et al. 1999, Moir et al. 2000). It has been shown to aid in the

localization of other nuclear proteins, and, as opposed to B-type lamins, lamin A is only observed in differentiated cells (Burke and Stewart 2002).

This mutation which causes HGPS is silent (G608G, GGC > GGT), but it alters a cryptic splice site to more closely resemble the consensus splice donor (Eriksson et al. 2003). The significance of alternate splicing is in the localization of the protein because post-translational maturation of lamin A includes farnesylation of the carboxyl terminus (Broers et al. 1999). The farnesylated prelamin A is processed by Zmpste24 which cleaves the C-terminus (Burke and Stewart 2002). In contrast, the alternate splice triggered in HGPS causes a 50 aa internal deletion, including the Zmpste24 recognition site, with the result that the polypeptide remains farnesylated. *In situ* progerin remains associated with the nuclear membrane and forms aggregates during mitosis instead of distributing evenly around the lamina (as wild type lamin A does); cells so affected develop nuclear blebs and invaginations (Glynn and Glover 2005, Wu et al. 2014).

HGPS serves as a model for what may be called the "aging phenotype." In addition to the aforementioned medical phenotypes, HGPS cells also maintain a higher frequency of DSBs over wild-type cells (Constantinescu et al., 2010). Even in non-HGPS cells, progerin concentration has been observed to increase with age (Verdy et al. 2011), and progerin expression correlates with nuclear deformations (Cao et al. 2007).

In this thesis, a model system mimicking progeria was created for the purpose of studying the effect of progerin upon repair of double-strand breaks. Plasmids were engineered for the expression of progerin under the regulation of a doxycycline-sensitive promoter. Furthermore, immortalized human fibroblasts were stably transfected with constitutively active progerin. These cells also contained a stably-integrated, inducible, selectable break repair substrate. Cells were cultured under selection to observe the results of repair of spontaneous and induced DNA double-strand breaks. It was hypothesized that the presence of progerin would increase the rate of error-prone repair events relative to higher fidelity events.

Chapter 2: Materials and Methods

Cell Lines

Cell line pLB4/11, described previously (Wang et al. 2011), was derived from SV40-immortalized normal human fibroblast cell line GM637 (obtained from the NIGMS) and contains a single integrated copy of recombination substrate pLB4 (Fig 2.1, example repair events shown in Fig 2.2). This plasmid contained a copy of herpes simplex virus 1 thymidine kinase fused to *neo*. The *tk* gene is interrupted by a 22 bp insertion which includes the I-SceI recognition site (Fig 2.3). The insert inactivates *neo* by causing a frame shift that reveals an early STOP codon. Upstream of the fusion gene is a second *tk* gene, which serves as a donor for repair of the fusion gene by HR. The donor differs from the recipient at 13 bases; these differences serve to identify the method of repair when repair products are sequenced.

HGADFN155 and HGADFN370 fibroblasts derived from HGPS patients were obtained from the Progeria Research Foundation, Peabody, MA, as were HGMDFN371 fibroblasts which were derived from an unaffected parent of HGADFN370.

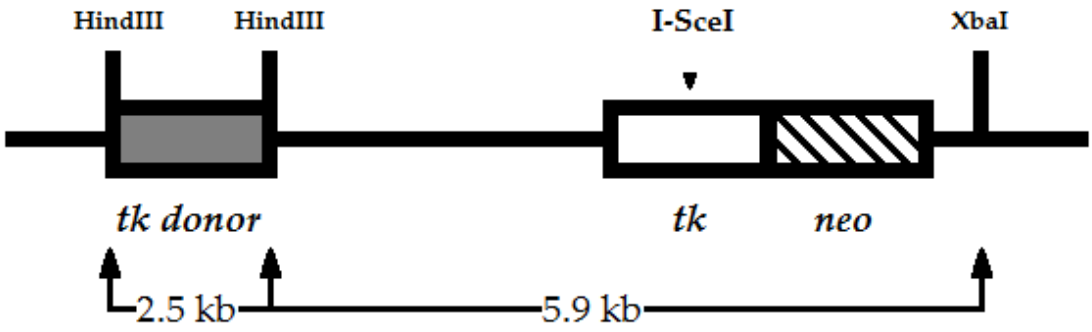

Figure 2.1 **The tk/neo Fusion Recombination Substrate Plasmid pLB4**

See text for details.

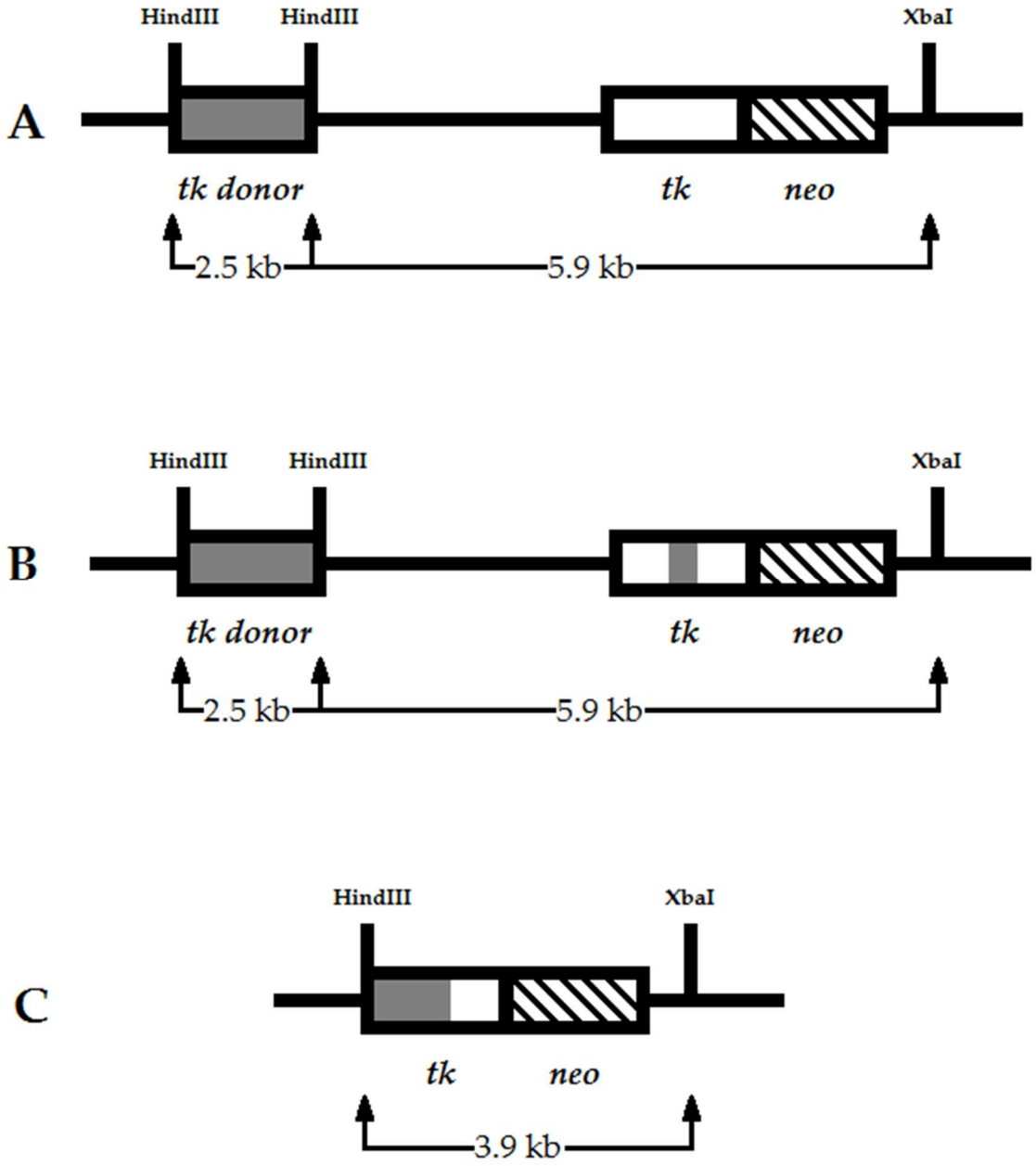

Figure 2.2 Repair of the tk/neo Fusion Recombination Substrate

A: The tk/neo fusion gene after an example NHEJ event. NHEJ events are not fully predictable and may result in large deletions which significantly decrease the distance between the second HindIII site and the XbaI site. **B:** The fusion gene after GC. Note the absence of the I-SceI site and the replacement sequence from the donor (variable in length). **C:** The fusion gene after CO or SSA. See text for details.

Figure 2.3 Inactivating Insert into tk/neo Fusion Gene.

This 22 bp insert forces a frame shift in the tk/neo fusion gene which also reveals an early STOP codon, inactivating G418 resistance. The box indicates the 18 bp recognition site for endonuclease I-SceI, and the arrows mark the location of the cut.

Cell Culture Conditions

Cells were cultured in minimal essential media, alpha modification (α-MEM) with 10% heat-inactivated fetal bovine serum and incubated at 37^{O}C in humidified 5% CO_2 air mixture.

Plasmids

pBABE-puro-GFP-progerin: This plasmid was a gift from Tom Misteli (Addgene plasmid #17663) (Fig 2.4). The plasmid contains an ampicillin resistance gene to enable selection during bacterial amplification of the plasmid and a puromycin resistance gene for selection in mammalian cells.

pBABE-puro-GFP: This plasmid is the result of digesting pBABE-puro-GFP-progerin with SalI (Fig 2.5). The smaller, D50-laminA, fragment (2.4 kb) was discarded, and the vector (5.9 kb) was ligated.

pTRE3G: Obtained from Clontech Laboratories, Inc., this plasmid is an empty vector designed to place a gene of interest under the regulation of promoter P_{TRE3G} (Fig 2.6). The promoter does not respond to mammalian transcription factors but will respond to transducible protein Tet-Express (631177, Clontech) according to protocols provided by Clontech Laboratories Inc. This plasmid also contains an ampicillin resistance gene to enable selection during bacterial amplification of the plasmid.

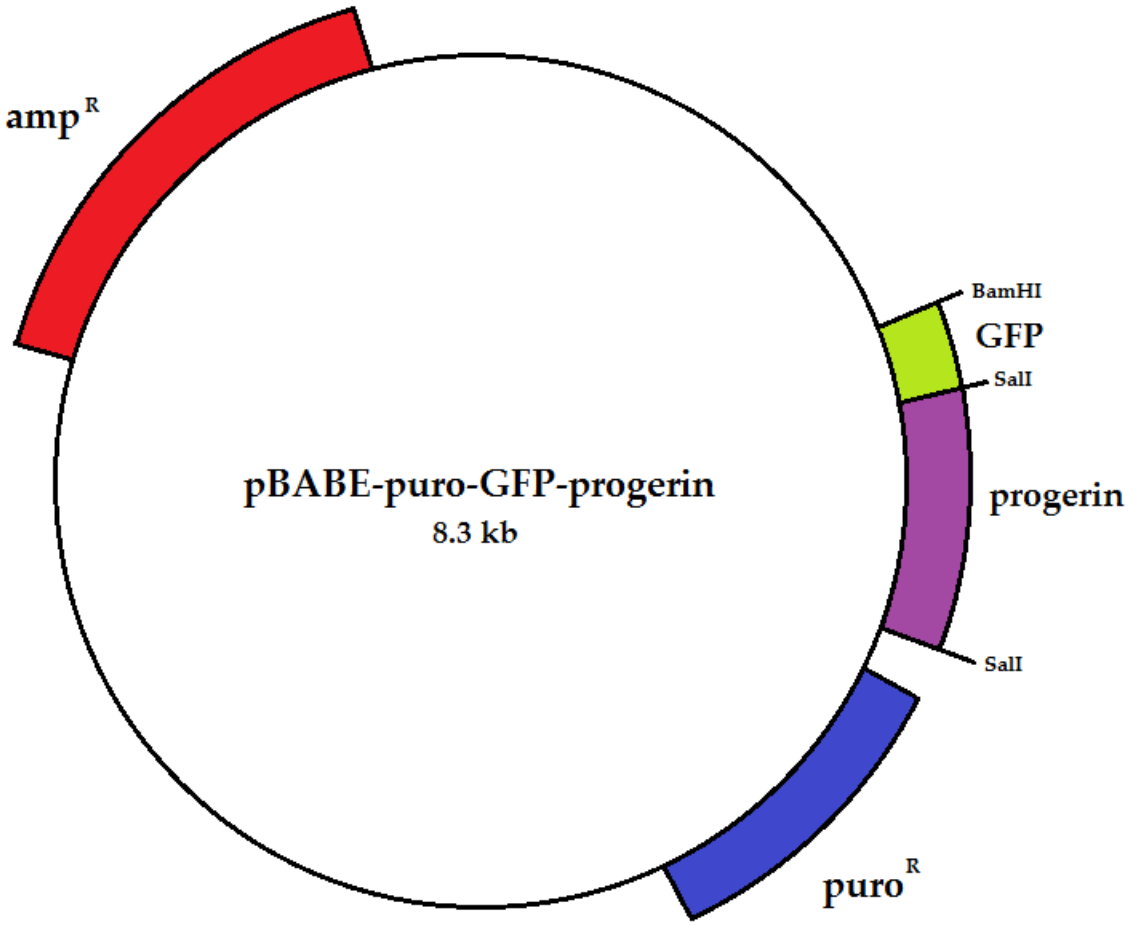

Figure 2.4 Plasmid pBABE-puro-GFP-progerin.

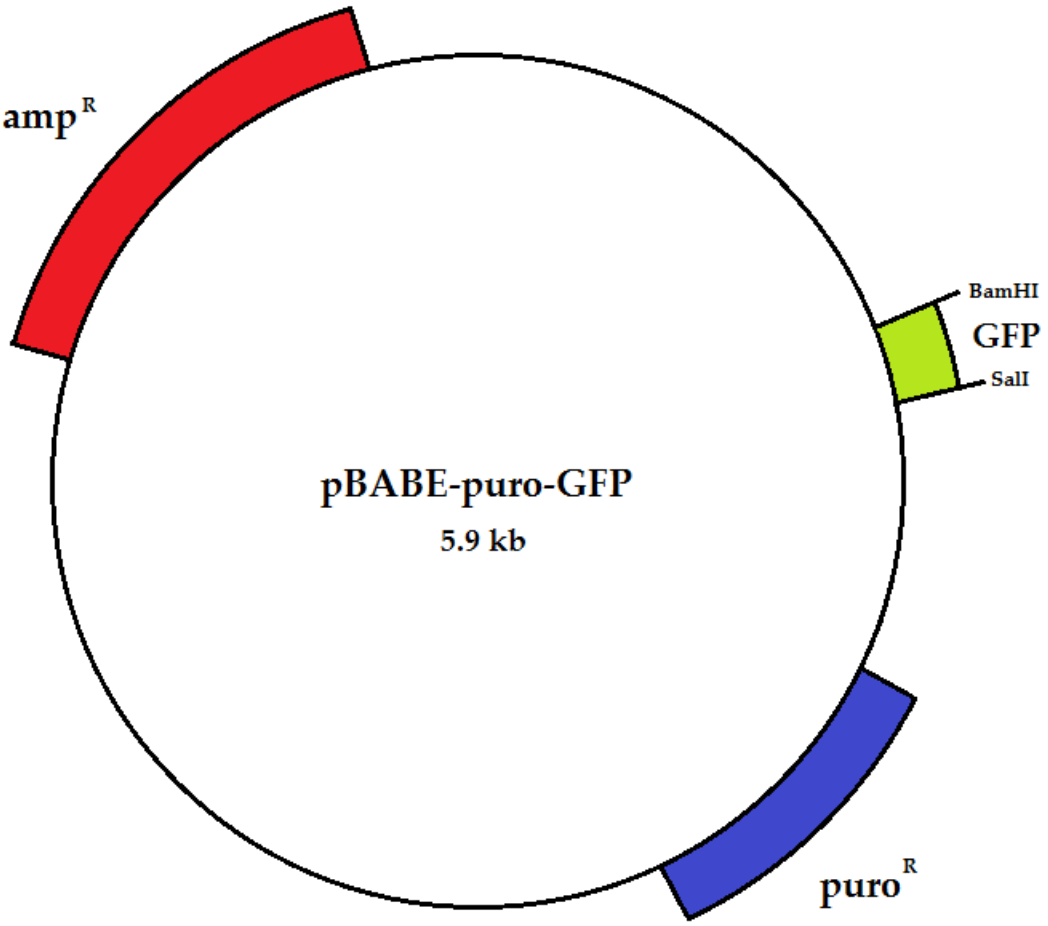

Figure 2.5 Plasmid pBABE-puro-GFP

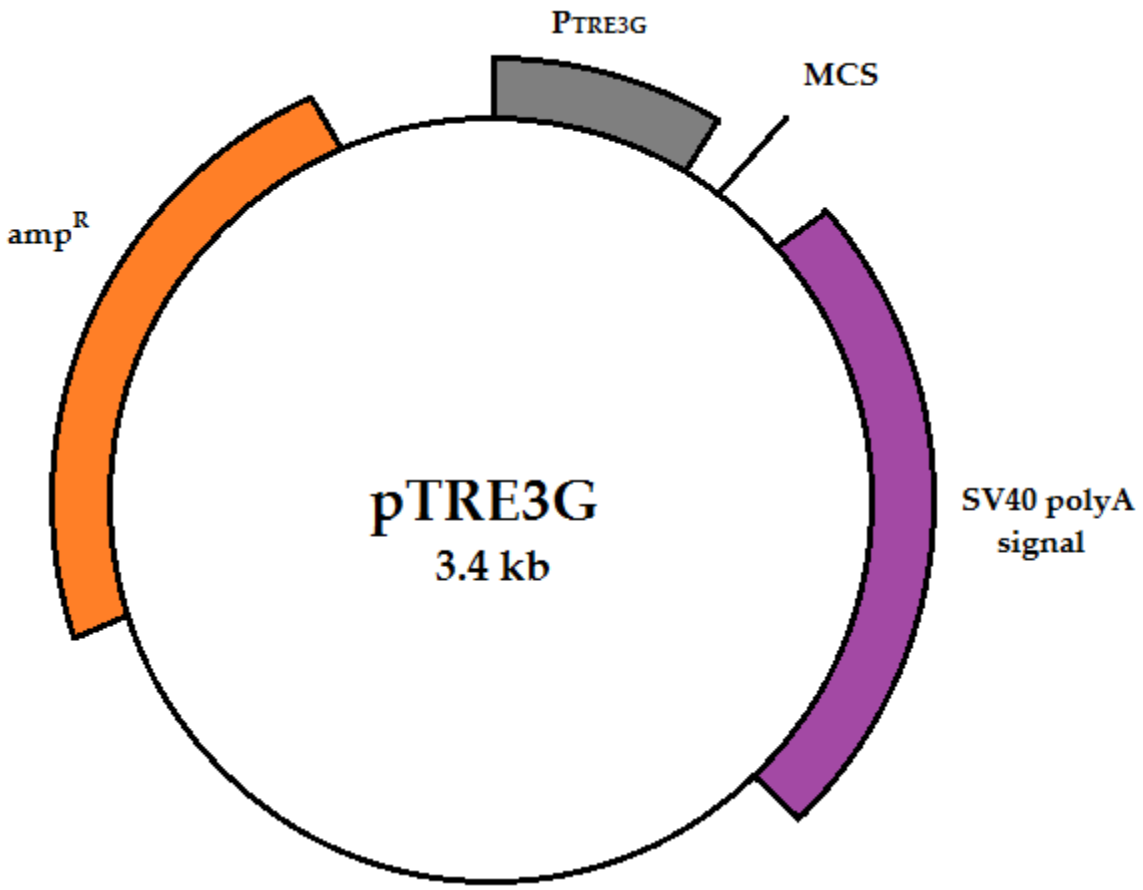

Figure 2.6 Plasmid pTRE3G

pCMV-3xnls-I-SceI: Obtained through the generosity of M. Jasin (Sloan Kettering), this plasmid (hereafter pSce) contains the gene for yeast endonuclease I-SceI. The N-terminus has been affixed with 3 copies of a nuclear localization signal. Plasmid pSce is used for transient expression of the endonuclease and is not intended to stably integrate.

pEGFP-D50-laminA: This plasmid was a gift from Tom Misteli (Addgene plasmid #17653) (Fig 2.7). The plasmid is derived from pEGFP-N1 (Fig 2.8) and includes a fusion gene of GFP and D50-laminA, an alternate name for progerin referring to the 50 aa deletion distinguishing it from wt laminA.

Restriction Enzyme Digests

All enzymes were acquired from New England Biolabs Inc. Restriction enzymes used included BamHI (R0126L), HindIII (R0104L), NheI (R0131S), NotI (R0189S), SalI (R0138S), and XbaI (R0145S). Restriction digests were conducted as prescribed by the supplier.

Agarose gel electrophoresis

Gel electrophoresis of DNA was performed using gels cast at 0.8% agarose and 0.05% ethidium bromide in TAE buffer (40 mM tris base, 20 mM acetate, 1 mM EDTA). The mass of sample was combined with 2 μL of dye and diluted with water to a final volume of 12 μL. Dilute samples were loaded into the gel alongside a combination of λ DNA-HindIII and φX174 DNA-HaeIII used ladder

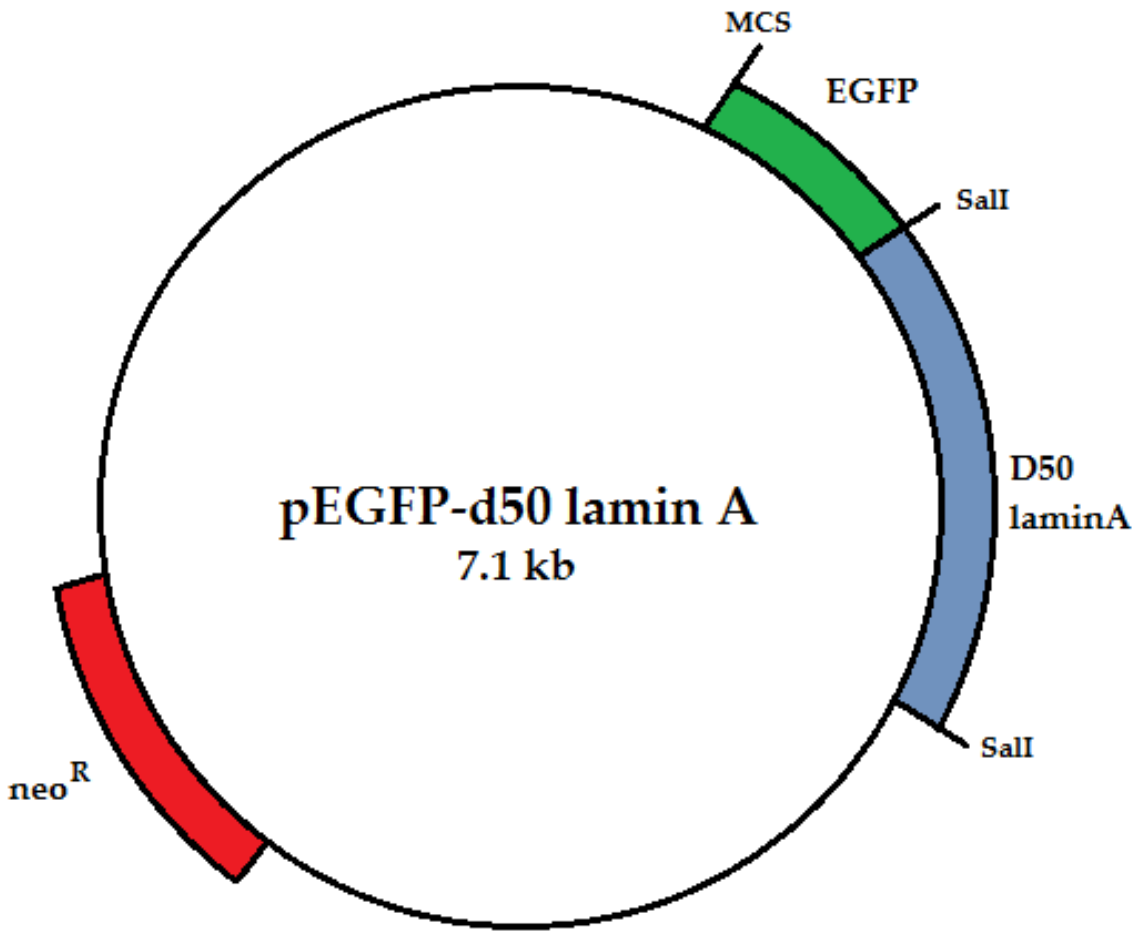

Figure 2.7 Plasmid pEGFP-D50-laminA

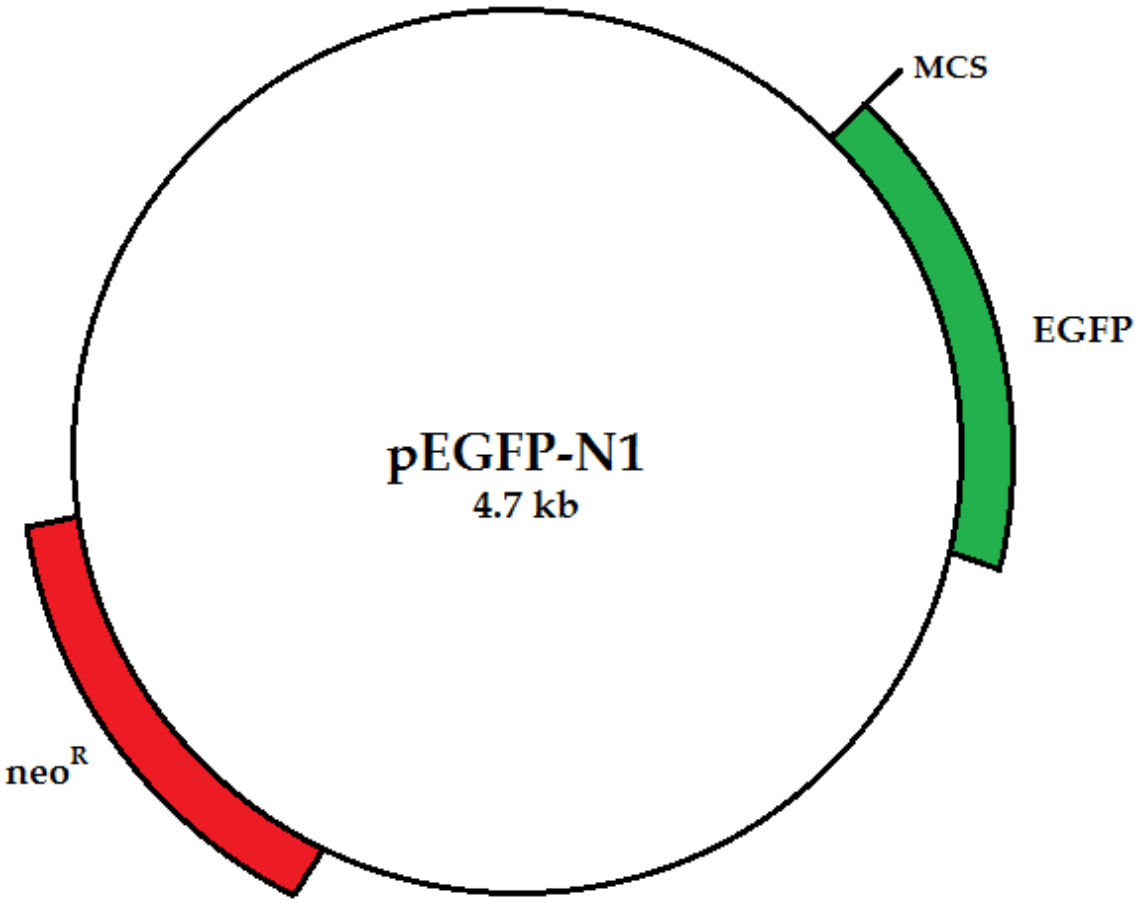

Figure 2.8 Plasmid pEGFP-N1

and run at 90 V for approximately 90 min. (precise time varied depending upon size of bands to be viewed) in TAE buffer with 0.05% ethidium bromide. Bands were visualized by exposure to UV radiation on a UVP transilluminator, and photographs were taken with a Polaroid MP4 LAND Camera.

Extraction of DNA from low melting point agarose gel

Low melting point agarose gels were cast at 0.9% (low melting point agarose, A-9414, Sigma-Aldrich Co. LLC) with 0.05% ethidium bromide in TAE buffer. The full digestion product was loaded across multiple lanes and run at 50 V for at least 2 hr. (until the bands separated). The desired band was cut from the gel and placed into a microcentrifuge tube for 10 min. incubation at 65^{O}C. The melted sample was then combined with an equal volume of Tris-equilibrated phenol and vortexed thoroughly. The sample was incubated on ice for 5 min. before centrifugation at 14,000 rpm in an Eppendorf Microcentrifuge 5415C. The resulting aqueous phase was transferred to a separate microcentrifuge tube and mixed with 3 volumes of 95% ethanol and 1/10th volume of 3M sodium acetate. This mixture was vortexed and then incubated at 80^{O}C for 10 min. Thereafter, it was centrifuged for 7 min., and the supernatant was discarded. The pellet was rinsed in 200 μL of 70% ethanol and then centrifuged once more for 5 min. The ethanol was removed by pipetting, and the sample was dried under vacuum at 60^{O}C in a Labconco Centrivap Concentrator

for 5 min. The dry pellet was resuspended in 20 μL of TE buffer (10 mM tris HCl at pH 8.0, 1 mM EDTA).

Plasmid construction

pTRE3G-GFP-progerin: Plasmid pTRE3G was digested with BamHI and NheI, yielding a 3.4 kb fragment and a smaller fragment of only 12 bases. The 3.4 kb fragment (the vector) was isolated by gel extraction. Plasmid pEGFP-D50-laminA was digested with BamHI and NheI to yield 4.7 and 3.2 kb fragments, of which the 3.2 kb fragment (containing D50-laminA) was also isolated by gel extraction. The pTRE3G fragment was treated with bacterial alkaline phosphatase (BAP, Thermo Fisher Scientific Inc. 18011-015) to prevent dimerization of the vector. The treated vector was then combined with the insert 1:1 by molarity, T4 DNA ligase (New England BioLabs Inc. M0202S), and ligase buffer (New England BioLabs Inc. B0202S) and incubated at 20^{O}C overnight. Ligation products were transformed into bacteria on ampicillin media to select for successful transformation.

pTRE3G.Sal⁻: Plasmid pTRE3G was digested with SalI. The linearized plasmid was blunted using NEB Quick Blunting Kit (E1201, New England Biolabs, Inc.). Blunted plasmid was recovered by gel extraction and ligated by T4 DNA ligase (Fig 2.9). Ligation products were transformed into bacteria on ampicillin media to select for successful transformation.

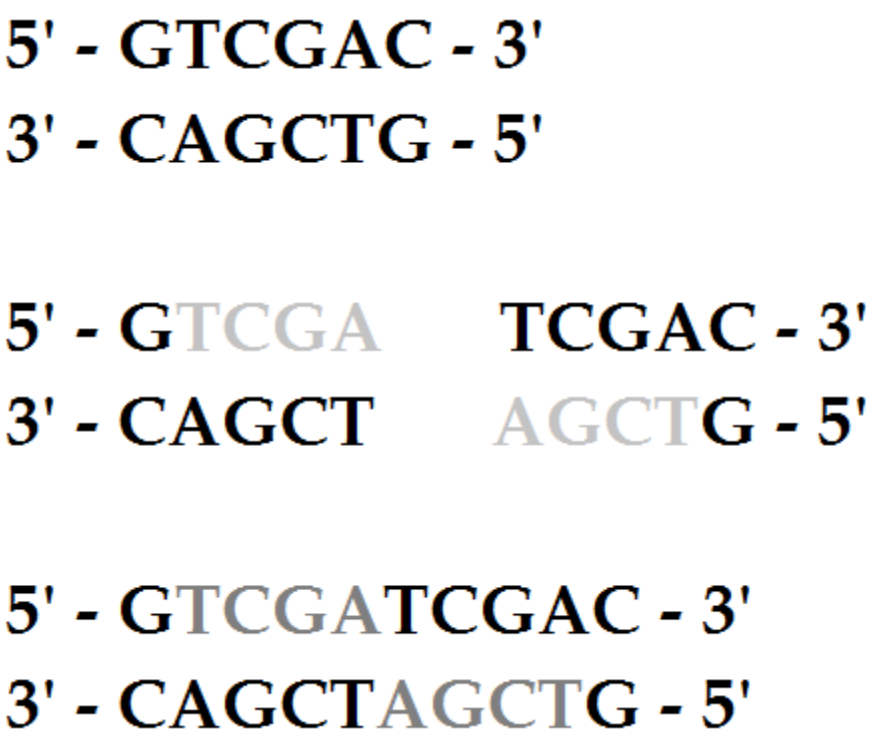

Figure 2.9 Destruction of SalI Restriction Site by Blunting and Ligation

Note that the ligation product no longer possesses a "GTCGAC" motif.

pTRE3G.Sal$^-$-GFP-progerin: The protocol to construct pTRE3G-GFP-progerin was repeated using pTRE3G.Sal$^-$ as the starting substrate.

pTRE3G-SΔS-GFP-progerin: Plasmid pTRE3G.Sal$^-$-GFP-progerin was digested with BamHI and treated with BAP as above. The linearized plasmid was combined with a BamHI to SalI adaptor sequence (Fig 2.10) at a ratio of 1:100 by molarity and ligated as above. Ligation products were transformed into bacteria on ampicillin media to select for successful transformation.

pTRE3G-SΔS-GFP: Plasmid pTRE3G-SΔS-GFP-progerin was digested with SalI. The larger fragment (4.2 kb) was isolated by gel extraction and ligated as above. Ligation products were transformed into bacteria on ampicillin media to select for successful transformation.

pTRE3G-SΔS-GFP-laminA: Plasmid pTRE3G-SΔS-GFP-progerin was digested with SalI. The larger 4.2 kb fragment (the vector) was isolated by gel extraction and treated with BAP as above. Plasmid pBABE-puro-GFP-laminA was digested with SalI, and its 2.4 kb fragment (laminA) was isolated by gel extraction. The vector and insert were combined 1:1 by molarity and ligated as above. Ligation products were transformed into bacteria on ampicillin media to select for successful transformation. Plasmid DNA was extracted from several bacterial colonies, and all were tested by two separate instances of diagnostic PCR to determine orientation of the insert. DNA was combined with GE

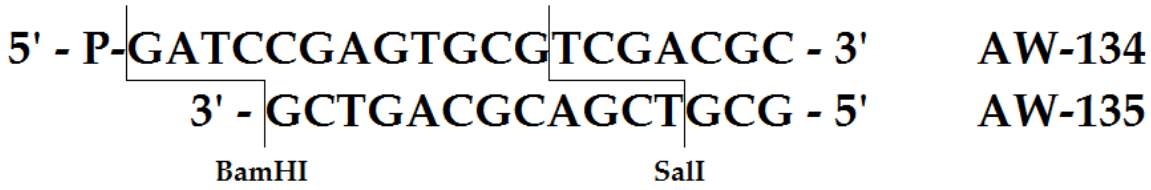

Figure 2.10 BamHI to SalI Adaptor

Oligonucleotides AW-134 and AW-135 were annealed to form this structure. AW-134 possesses a 5′ phosphate to permit binding to an existing BamHI sticky end. The SalI site is not revealed until it has been digested.

Healthcare illustra PuReTaq Ready-To-Go PCR beads and primers AW-136/AW-137 or AW-136/AW-138 (forward or reverse product, Fig 2.11) and subjected to touchdown PCR. Initial denaturation was for 5 min. at 95^{O}C followed by 14 cycles of 1 min denaturation (95^{O}C), 1 min. annealing, and 3 min. elongation (72^{O}C). Annealing temperature started at 72^{O}C and dropped by 2^{O}C every 2nd cycle to a final temperature of 60^{O}C. Protocol was conducted using a Perkin Elmer DNA Thermal Cycler. PCR products were visualized by gel electrophoresis to determine which reaction yielded product.

Amplification of plasmids in bacterial cultures

Amplifications were conducted using Bioline α-Select Gold Efficiency Chemically Competent Cells (BIO-85027) for amplification. For each plasmid, plasmid solution was mixed with bacterial solution and processed according to the supplier's protocol. During selection steps, cells were cultured in media with 100 μg/mL ampicillin.

Purification of plasmids from bacterial cultures

Plasmids were purified from bacteria using the QIAprep Spin Miniprep Kit (27104). Extractions were performed according to the instructions provided with the kit, including buffers provided. Centrifugations were conducted in an Eppendorf Microcentrifuge 5415C.

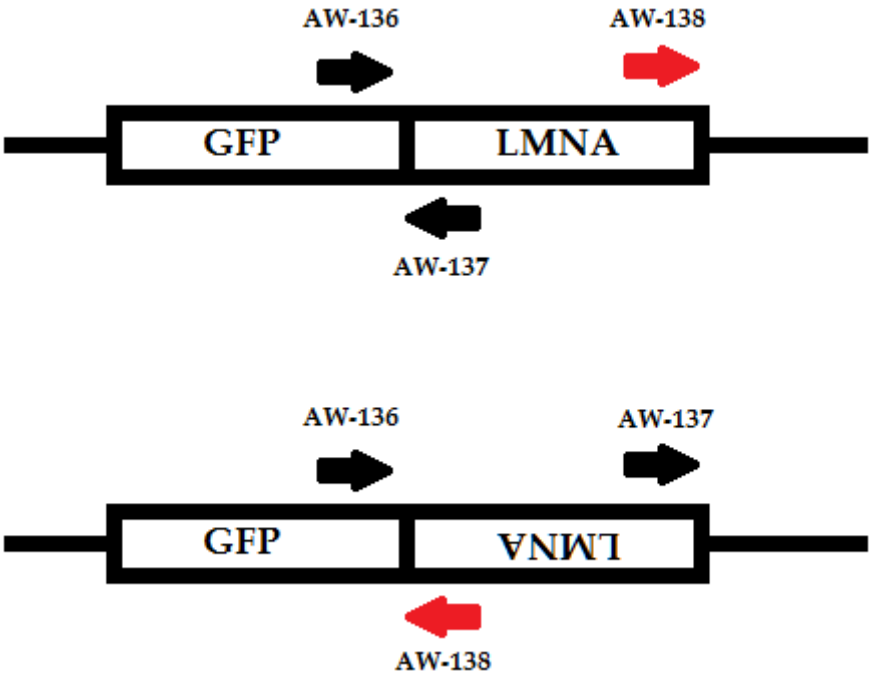

Figure 2.11 Orientation of LMNA when Inserted into pTRE3G-SΔS-GFP

PCR amplification with primers AW-136 and AW137 yields product in plasmids with the correct orientation of LMNA. AW-136 and AW-138 yield product in plasmids with reverse orientation.

Establishment of stable human cell lines integrated with pBABE derivatives

Transfections were accomplished by electroporation. Five million cells of the desired cell line were suspended in 800 μL of PBS with 5 μg of the desired plasmid (pBABE-puro-GFP or pBABE-puro-GFP-progerin, linearized by digestion with NotI) and electroporated using a Bio-Rad Gene Pulser set to 700 V and 25 μFd. The cells were then cultured in a 175 cm^2 flask for 48 hr. to recover from stress.

To identify and isolate resistant clones, cell lines were cultured into media with 0.5 μg/mL puromycin. The cultures were established at densities of 10^6 cells per 75 cm^2 flask. After a suitable growth period (between 14 and 21 days, depending upon individual ability to thrive), colonies were counted and then picked and cultured individually.

Cultures were screened for GFP expression by viewing under an EVOS fl Cell Imaging System (Thermo Fisher Scientific). Cell lines judged to have high levels of expression were subjected to protein extraction for later analysis by Western blot.

Protein Extraction

Cell cultures used for protein extraction were grown to confluence in 25 cm^2 flasks. After aspirating the medium and rinsing with 5 mL PBS, cells were detached from the flask by incubation in 500 μL trypsin-EDTA. The loose cells

were resuspended in 4.5 mL medium and transferred to a conical tube for 3 min. of centrifugation in a Clay Adams Dynac Centrifuge (Beckton, Dickinson and Company) at a speed setting of "40". Medium was aspirated, and the cells were resuspended in 10 mL PBS at 4°C. The above centrifugation was repeated, and existing PBS was aspirated before resuspending the cells in 1.5 mL PBS, again 4°C. This suspension was transferred to a microcentrifuge tube for 5 min. centrifugation at 4000 rpm and 4°C in an Eppendorf Microcentrifuge 5415 R. After once more aspirating the PBS, the cells were resuspended in 100 μL RIPA buffer (50 mM tris, 150 mM NaCl, 0.1% SDS, 0.5% sodium deoxycholate, 1% Triton X 100) with protease inhibitor (P8340-1ML, Sigma-Aldrich Co. LLC). Samples were incubated on ice for 30 min. and then centrifuged for 10 min. at 10,000 rpm and 4°C. The supernatant was collected for further use, and the precipitate was discarded.

Protein concentration assay

Concentration of protein extracts was determined by comparison against a series of BSA standards from 0 to 0.8 μg/μl in RIPA buffer. The standards and a 1:10 dilution of each of the samples (total volume 20 μL) were individually mixed into 1 mL of dilute dye reagent (Bio-Rad Protein Assay Dye Reagent Concentrate, #500-0006). The dye reagent was prepared by diluting the concentrate 1:5 in water and filtering with Whatman paper. Samples with dye

were mixed by vortexing and then incubated for 5 min. at room temperature. Sample absorbances were measured at 595 nm using a Hitachi U-2000 Spectrophotometer. All samples were performed in duplicate, and the average absorbance was compared against the slope of the trend line provided by the BSA standards.

Western blotting

Polyacrylamide gels used for western blots were cast using 8% separating gels (800 μL 40% acrylamide/bis (29:1), 1 mL tris/SDS (pH 8.8), 40 μL 10% ammonium persulfate, 6.5 μL TEMED) and 4% stacking gels (250 μL 40% acrylamide/bis (29:1), 625 μL tris/SDS (pH 8.8), 25 μL 10% ammonium persulfate, 6 μL TEMED). Cellular protein extract (30 μg) was diluted to 10 μL with RIPA buffer with an additional 2 μL of SDS sample buffer with dye (300 mM Tris-HCl, 12% SDS, 30% glycerol, 0.06% bromophenol blue, 600 mM DTT). The samples were heated for 5 min. at 95^{O}C before loading into the gel. The Bio-Rad Precision Plus Kaleidoscope Protein Standard (#161-0375, 5 μL) was used as marker, and gels were run in a Bio-Rad Mini Protean 3 Cell assembly (running buffer: 25 mM tris base, 192 mM glycine, 0.1% SDS w/v).

Gels were run at 14 mA until all samples passed out of the separating gel (as observed from dye front). Thereafter, gels were run at 18 mA for approximately 90 min. After electrophoresis, the stacking gels were detached

and discarded, and the separating gels were packed into a transfer assembly with a 60 mm x 80 mm x 0.45 μm Amersham Hybond ECL nitrocellulose membrane (RPN68D). Transfers were performed in transfer buffer (25 mM tris base, 192 mM glycine, 20% v/v methanol) on ice at 100 V for 90 min. The membrane was blocked overnight by 40 rpm shaking at 4^{O}C in 70 mL of blocking buffer (10 mM tris HCl, 150 mM NaCl, 0.1% v/v polysorbate 20, 5% w/v non-fat dry milk).

After blocking buffer was drained, the membrane was incubated in the primary antibody diluted in the same blocking buffer. Primary antibodies used were GFP (B-2): sc-9996 (mouse monoclonal, from Santa Cruz Biotechnology, Inc.) at a dilution of 1:500, Lamin A/C (N-18): sc-6215 (goat polyclonal, from Santa Cruz Biotechnology, Inc.) at a dilution of 1:500, and Anti-Progerin antibody [13A4] ab66587 (mouse monoclonal, from Abcam Inc.) at a dilution of 1:1000. Incubation was for 60 min. at 45 rpm and 4^{O}C. Afterwards, the membrane was rinsed four times with wash buffer (10 mM tris HCl, 150 mM NaCl, 0.1% v/v polysorbate 20) and then incubated in fresh wash buffer with 90 rpm shaking at 4^{O}C four times, 5 min. each time. This was followed by incubation in secondary antibody. Secondary antibodies used were goat anti-mouse IgG-HRP: sc-2005 (Santa Cruz Biotechnology, Inc.) at a dilution of 1:1000 and donkey anti-goat IgG-HRP: sc-2020 (Santa Cruz Biotechnology, Inc.) at a

dilution of 1:5000. Incubation was likewise 60 min. at 45 rpm and 4^{O}C, and this was followed by another cycle of rinse and wash as described above.

Detection was accomplished using GE Healthcare Amersham ECL Select Western Blotting Detection Reagent. Component solutions A and B were mixed in equal quantities (1 mL of each per 24 cm^2 of membrane), spread evenly over the membrane surface, and allowed to incubate for 5 min. at room temperature. Imaging was conducted using a GE ImageQuant LAS 4000 courtesy of Dr. Beth Krizek, University of South Carolina.

Selection for repair of induced DSB

To test for the effect of progerin on the rate of DSB repair, cells containing stably integrated pBABE derivatives were transiently transfected with pSce. Five million cells of the desired cell line were suspended in 800 μL of PBS with 20 μg pSce and electroporated using a Bio-Rad Gene Pulser set to 700 V and 25 μFd. The cells were then cultured in a 175 cm^2 flask for 48 hr. to recover from stress.

To identify and isolate resistant clones, cell lines were cultured into media with 1000 μg/mL active G418. The cultures were established at densities of 10^4, 10^5, and 10^6 cells per 75 cm^2 flask to ensure individual colonies could be isolated. After a suitable growth period (between 14 and 21 days, depending upon individual ability to thrive), colonies were counted and then picked and cultured individually.

Selection for spontaneous repair events

Additional cells were cultured under selection without pSce transfection to test for spontaneous events. Cells were cultured into media with 1000 μg/mL active G418 at a density of 10^6 cells per 75 cm^2 flask. The sub-clones were subjected to fluctuation analysis using protocol described previously (Waldman and Liskay 1988).

Extraction of genomic DNA from cell culture

Cells were grown to confluence in a 75 cm^2 flask and then subjected to a genomic DNA extraction protocol modified from Liskay and Evans (1980). The flask was aspirated of its medium and then washed with 10 mL of PBS. The PBS, also, was aspirated, and the flask was incubated with 2 mL of lysis buffer and 35 μL of 10 mg/mL Proteinase K (BMB #161519 in TE buffer) for 10 min. The resulting slurry was transferred to a polypropylene tube and incubated at 56^{O}C overnight. Tris-equilibrated phenol (2.5 mL) was mixed into the lysate by 1 min. of vortexing and then separated by centrifugation for 10 min. in an IEC HN-SII Centrifuge set to 88% speed. The aqueous phase and interface material were transferred to a new tube for vigorous mixing with 2.5 mL ether. The mixture was then centrifuged for 5 min. whereupon the ether phase was removed by pipetting. Residual ether was removed by permitting the sample to incubate for 3 min. while exposed to atmosphere. DNA was precipitated by adding 200 μL of

3M sodium acetate (pH 6.0) and 2 mL of 95% ethanol at 0^{O}C. The sample tube was inverted repeatedly until DNA began to precipitate into a fine, gauze-like appearance. DNA was spooled onto a borosilicate pipette and dipped into 70% ethanol to rinse. The pipette tip with DNA was broken off into a microcentrifuge tube and dried under vacuum at 60^{O}C in a Labconco Centrivap Concentrator for 3 min. DNA was resuspended in 200 μL TE with 1.8 μL Ambion RNAse cocktail (AM2286) and incubated at 37^{O}C overnight.

The sample was subjected to a second phenol extraction. After mixing by vortexing, 200 μL of phenol was added to the sample, which was vortexed again (1 min.) to mix. The sample was centrifuged at 14,000 rpm in an Eppendorf Microcentrifuge 5415C for 2 min., and then the aqueous phase (and interface material) were transferred to a new microcentrifuge tube. Ether was added (1 mL) and mixed into the sample by 1 min. of vortexing. The sample was separated by centrifugation at 14,000 rpm for 2 min. Thereafter, the ether phase was removed by pipetting, and residual ether was dried off by exposing the sample to atmosphere for 3 min. DNA was precipitated by adding 133 μL of 7 M ammonium acetate and 833 μL of 95% ethanol (both at 0^{O}C) and inverting the sample repeatedly. The sample was then centrifuged for 5 min. at 14,000 rpm. Supernatant was removed by decanting, and the pellet was rinsed with 200 μL of 70% ethanol. After a further 3 min. of centrifugation, the ethanol was removed

by pipetting, and the pellet was dried under vacuum at 60^{O}C in the Centrivap for 3 min. The pellet was resuspended in 180 μL TE and incubated at 37^{O}C overnight.

DNA concentration assay

Genomic DNA collected from extractions was diluted 1:20 in TE buffer. Duplicate 60 μL aliquots of the dilute DNA were measured for absorbance at 260 nm and 280 nm with a Hitachi U-2000 Spectrophotometer. Sample purity was judged according to the ratio of absorbance A_{260}/A_{280} (expected value 1.8). Absorbances of the duplicates were averaged. Due to the dilution factor, A_{260} values were equal to the concentrations of the undiluted samples expressed in units of μg/μL.

DNA sequencing

Genomic DNA was combined with GE Healthcare illustra PuReTaq Ready-To-Go PCR beads and primers AW85 and AW91 (Fig 2.12, amplification locus shown in Fig 2.13) and subjected to touchdown PCR, described above. Protocol was conducted using a Perkin Elmer DNA Thermal Cycler. PCR products were then treated with Exonuclease I (Affymetrix, Inc. part 70073X, 1 unit/ 1 μL of sample) to eliminate primers and Shrimp Alkaline Phosphatase (Affymetrix, Inc. part 78390, 1 unit/ 10 μL of sample) to destroy residual nucleotides. Enzymes were inactivated by 15 min. incubation at 80^{O}C before

AW-85	**5'- TAATACGACTCACTATAGGGCCAGCGTCTTGTCATTGGCG -3'**
AW-91	**5'- GATTTAGGTGACACTATAGCCAAGCGGCCGGAGAACCTG -3'**

Figure 2.12 PCR Primers for Identification of DSB Repair Event by Sequencing

Primers AW-85 and AW-91 flank the region shown in Fig 2.13. Their amplification product may be used to determine the method of repair.

```
Recipient   1     ccagcgtcttgtcattggcgaattcgaacacgcagatgcagtcggggcggcgcggtccgagtgtggcctcga
Donor       1     ccagcgtcttgtcattggcgaattcgaacacgcagatgcagtcggggcggcgcggtcccagtgtggcctcga

Recipient   73    acaccgagcgaccctgcagcgacccgcttaacagcgtcaacagcgtgccgcagatcttggtggcgtgaaact
Donor       73    acaccgagcgaccctgcagcgacccgcttaacagcgtcaacagcgtgccgcagatcttggtggcgtgaaact

Recipient   145   ccggtccacttcgcatattaaggtgacgccgcacctcttcggccagcgccttgtagaagcgcgtatggcttc
Donor       145   ccggtccacttcgcatattaaggtgacgccgcacctcttcggcaagcgccttgtagaagcgcgtatggcttc

Recipient   217   gtaccccggccatcaacacgcgtctgcgttcgaccaggctgcgcgttctcgcggccatagcaaccgacgtac
Donor       217   gtaccccctgccatcaacacgcgtctgcgttcgaccaggctgcgcgttctcgcggccatagcaaccgacgtac

Recipient   289   ggcgttgcgccctcgccggcagcaagaagccacggaagtccgcctggagcagaaaatgcccacgctactgcg
Donor       289   ggcgttgcgccctcgccggcagcaagaagccacggaagtccgcctggagcagaaaatgcccacgctactgcg

Recipient   361   ggtttatatagacggtcctcacgggatggggaaaaccaccaccacgcaactgctggtggccctgggttcgcg
Donor       361   ggtttatatagacggtcctcacgggatggggaaaaccaccaccacgcaactgctggtggccctgggttcgcg

Recipient   433   cgacgatatcgtctacgtacccgagccgatgacttactggcaggtgctgggggcttccgagacaatcgcgaa
Donor       433   cgacgatatcgtctacgtacccgagccgatgacttactggcaggtgctgggggcttccgagacaatcgcgaa

Recipient   505   catctacaccacacaacaccgcctcgaccagggtgagatatcggccggggacgcggcggtggtaatgacaag
Donor       505   catctacaccacacaacaccgcctcgaccagggtgagatatcggccggggacgcggcggtggtaatgacaag

Recipient   577   cgcccagataacaatgggcatgccttatgccgtgaccgacgccgttctggctcctcatatcgggggggaggc
Donor       577   cgcccagataacaatgggcatgccttatgccgtgaccgacgccgttctggctcctcatgtcgggggggaggc

Recipient   649   tgggagcttagggataacagggtaatagctcacatgccccgcccccggccctcaccctcatcttcgaccgcc
Donor       649   tggg----------------------agttcacatgccccgcccccggccctcaccctcatcttcgaccgcc

Recipient   721   atcccatcgccgccctcctgtgctacccggccgcgcgataccttatgggcagcatgaccccccaggccgtgc
Donor       699   atcccatcgccgccctcctgtgctacccggccgcgcgataccttatgggcagcatgaccccccaggccgtgc

Recipient   793   tggcgttcgtggccctcatcccgccgaccttgcccggcacaaacatcgtgttgggggccctccggaggaca
Donor       771   tggcgttcgtggccctcatcccgccgaccttgcccggcacaaacatcgtgttgggggccctccggaggaca

Recipient   865   gacacatcgaccgcctggccaaacgccagcgccccggcgagcggctggacctggctatgctggctgcgattc
Donor       843   gacacatcgaccgcctggccaaacgccagcgccccggcgagcggcttgacctggctatgctggccgcgattc

Recipient   937   gccgcgtttacgggctacttgccaatacggtgcggtatctgcagtgcggcgggtcgtggcgggaggactggg
Donor       915   gccgcgtttacgggctgcttgccaatacggtgcggtatctgcagggcggcgggtcgtggcgggaggattggg

Recipient   1009  gacagctttcggggacggccgtgccgccccagggtgccgagccccagagcaacgcgggcccacgaccccata
Donor       987   gacagctttcggggacggccgtgccgccccagggtgccgagccccagagcaacgcgggcccacgaccccata

Recipient   1081  tcggggacacgttattaccctgtttcgggcccccgagttgctggcccccaacggcgacctgtataacgtgtt
Donor       1059  tcggggacacgttattaccctgtttcgggcccccgagttgctggcccccaacggcgacctgtacaacgtgtt

Recipient   1153  tgcctgggccttggacgtcttggccaaacgcctccgttccatgcacgtctttatcctggattacgaccaatc
Donor       1131  tgcctgggccttggacgtcttggccaaacgcctccgtcccatgcacgtctttatcctggattacgaccaatc

Recipient   1225  gcccgccggctgccgggacgccctgctgcaacttacctccgggatggtccagacccacgtcaccacccccgg
Donor       1203  gcccgccggctgccgggacgccctgctgcaacttacctccgggatggtccagacccacgtcaccacccccgg

Recipient   1297  ctccataccgacgatatgcgacct
Donor       1275  ctccataccgacgatctgcgacct
```

Figure 2.13 Sequence Alignment of HSV-1 tk Recipient and Donor Genes

In addition to the 22 bp I-SceI insert (the sequence in the recipient above with no counterpart in the donor), the donor and recipient sequences differ at 13 bases. These mismatches may be used to distinguish between repair events.

submitting samples for sequencing to Eton Bioscience Inc., Research Triangle Park, NC. Sequencing relies upon the T7 promoter incorporated into primer AW85.

Southern blotting

Genomic DNA from G418 resistant cultures was analyzed by Southern hybridization using a 32P-labeled probe specific for the HSV-1 tk sequence as described previously (Lukacsovich et al. 1994). Blots were exposed to Amersham Hyperfilm MP (GE Healthcare Limited, 28906845) and developed on a Futura Classic E Automatic X-Ray Film Processor (Fischer Industries Inc.).

Statistical Analysis

Statistical analysis was performed using a Pearson's chi-squared test of independence. Significance values were calculated using Simple Interactive Statistical Analysis (Uitenbroek 1997).

Chapter 3: Construction of Plasmids for Use in Modeling Progeria in Human Cell Lines

To establish cell lines for the study of the effect of inducible progerin upon DSB repair, plasmids were constructed based on pTRE3G (Fig 2.6). Genes inserted into the multicloning site of pTRE3G are under the regulation of P_{TRE3G}, a promotor with very low expression in mammalian cells. However, under conditions indicated by the supplier, P_{TRE3G} is strongly induced. Progerin was integrated into the plasmid under the regulation of this promoter, and GFP was appended as a fusion protein to serve as a marker for screening. It was decided that, in addition to the experimental GFP-progerin cell line, four control cell lines would be required: no vector, empty vector, GFP, and GFP-laminA. The empty vector controls for the presence of the plasmid, GFP for the presence of active synthesis from the plasmid, and GFP-laminA for whether observed effects were attributable to the defect within progerin or merely to the increase in nuclear lamins, since plasmid activity is in addition to, rather than instead of, native lamin A synthesis.

To construct plasmid pTRE3G-GFP-progerin, the multicloning site of pTRE3G was opened with BamHI and NheI, and a GFP progerin fragment derived from pEGFP-D50-laminA was inserted, placing fusion gene GFP-progerin under the regulation of P_{TRE3G}. Plasmids were amplified by transformation into bacteria, relying upon the ampicillin resistance provided by pTRE3G for selection (Fig 3.1 A). Correct construction was confirmed by extraction of plasmid DNA and digestion with BamHI and NheI. The correct plasmid yields two fragments, the 3.4 kb vector and the 3.2 kb GFP-progerin fusion gene (Fig 3.2).

The construction of a plasmid containing laminA was not straightforward due to the incompatibility of restriction sites among available plasmids. To surmount this difficulty, the existing SalI site of pTRE3G was destroyed by cutting at the restriction site, filling in the overhang, and ligating the blunt ends together (Fig 2.9), resulting in plasmid pTRE3G.Sal^- (Fig 3.1 B). This was done to prevent the existing SalI site from interfering with a later digestion.

Plasmid pTRE3G.Sal^- was digested with BamHI and NheI, and a GFP-progerin fragment derived from pEGFP-D50-laminA was inserted, placing fusion gene GFP-progerin under the regulation of P_{TRE3G}, as before. Plasmids were amplified by transformation into bacteria, relying upon the ampicillin resistance provided by pTRE3G for selection. Correct construction was

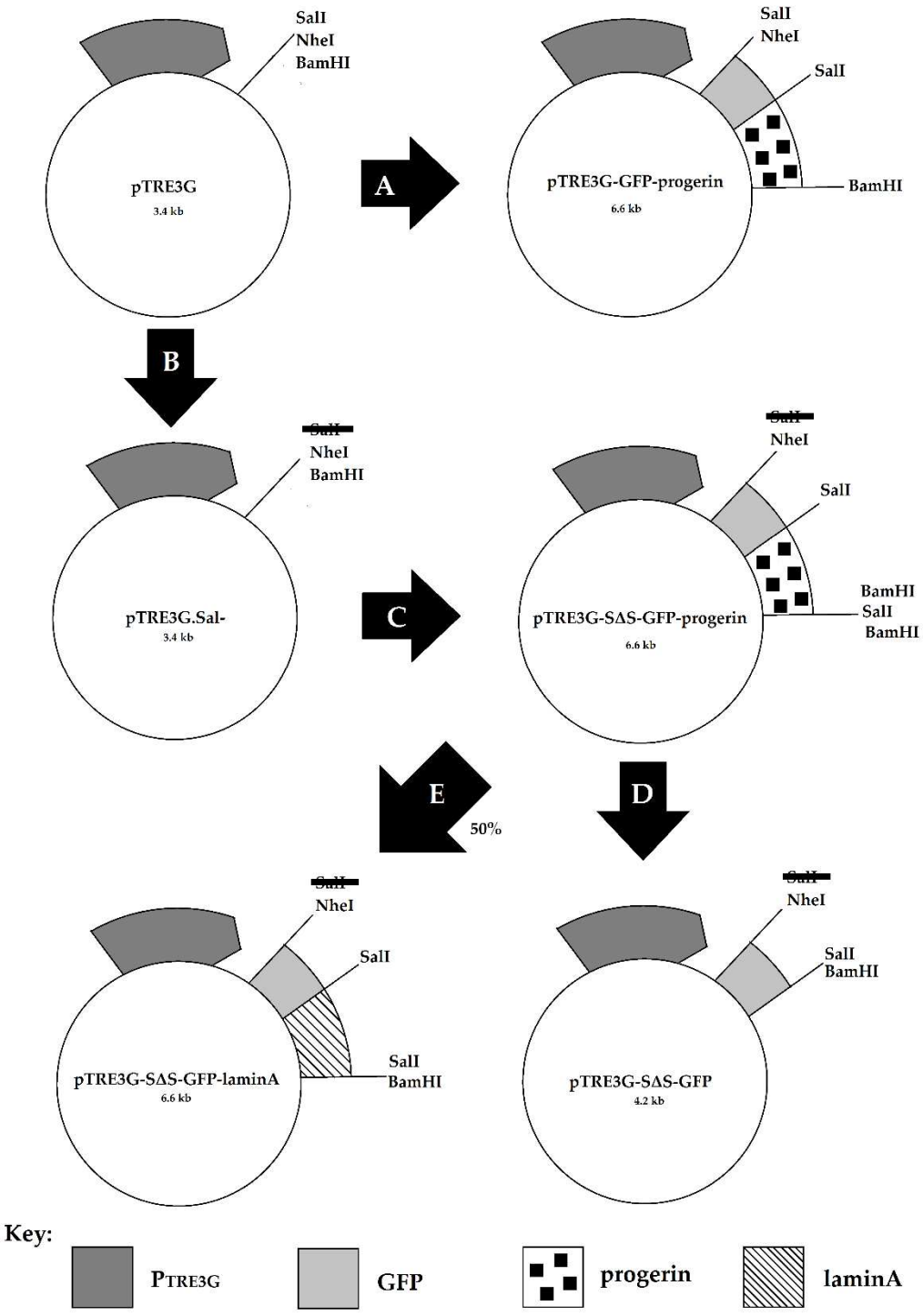

Figure 3.1 Schematic for Construction of pTRE3G Derivatives

See text for details.

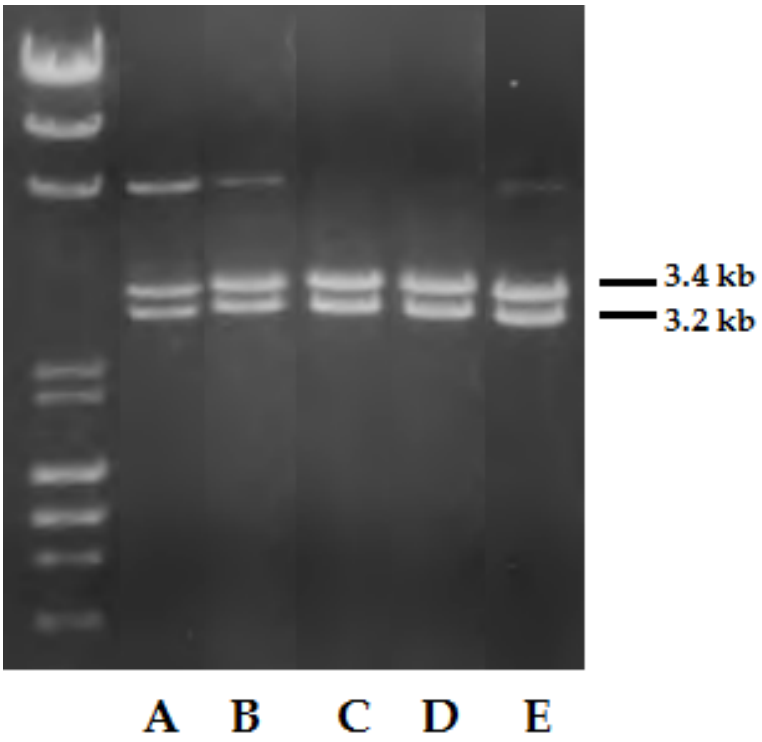

Figure 3.2 BamHI/NheI Digest of Potential pTRE3G-GFP-progerin Extracts

Lanes C and D show the smaller GFP-progerin band and the larger vector band and were kept as representative samples of plasmid pTRE3G-GFP-progerin. Lanes A, B, and E show an additional band, suspected to be singly cut plasmid, and were rejected. A combination of λ DNA-HindIII and φX174 DNA-HaeIII was used as ladder.

confirmed by extraction of plasmid DNA and digestion with BamHI and NheI. The correct plasmid yields two fragments, the 3.4 kb vector and the 3.2 kb GFP-progerin fusion gene. Following that, however, the BamHI site at the 3' end of the progerin gene was opened and an adaptor was added to give the locus a new SalI site (Fig 2.10). Combined with the way in which pEGFP-D50-laminA was constructed, this left the progerin gene of the pTRE3G.Sal- derivative flanked by SalI sites (now called pTRE3G-SΔS-GFP-progerin, Fig 3.1 C).

Plasmid pTRE3G-SΔS-GFP-progerin was digested by SalI. Gel extraction of the larger fragment and ligation without further ado results in pTRE3G-SΔS-GFP, one of the desired controls (Fig 3.1 D). Correct construction was confirmed by extraction of plasmid DNA and digestion with BamHI and NheI. The correct plasmid yields two fragments, the 3.4 kb vector and the 0.8 kb GFP gene (Fig 3.3). The GFP band is not visible due to its low total mass. Increasing the initial mass of DNA loaded into the gel reveals the formerly invisible band (Fig 3.4).

The isolated larger fragment from SalI digestion of pTRE3G-SΔS-GFP-progerin was also taken and combined with the smaller fragment from SalI digestion of pBABE-puro-GFP-laminA. This fragment contains only the lamin A gene; however, due to the identical restriction sites on both end of the fragment, the ligation is non-directional. Thus, when the plasmid was transformed into bacteria, several colonies were collected, all of which were subjected to plasmid

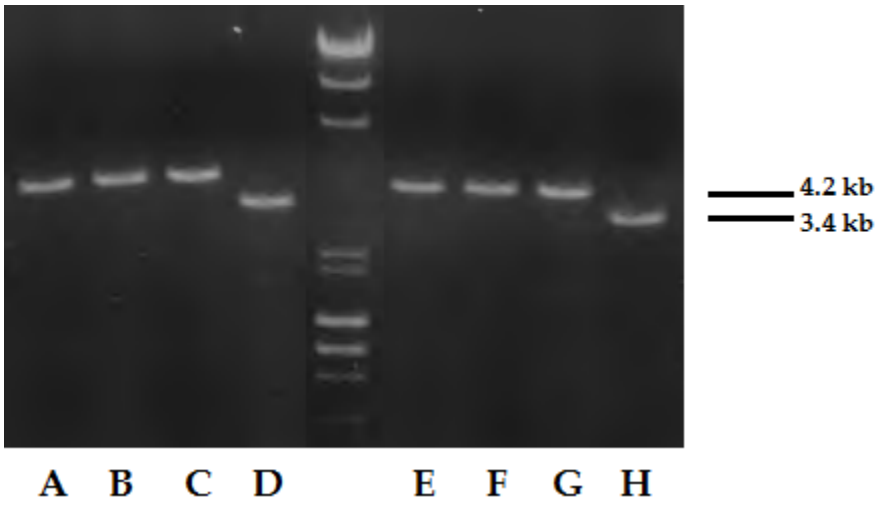

Figure 3.3 Multiple Digests of Potential pTRE3G-SΔS-GFP Extracts

The gel shows multiple digest products of 2 separate plasmid extractions. Lanes A-C and E-G are single digests by BamHI, SalI, or NheI, each of which recognizes only one restriction site on the expected plasmid. Lanes D and H are digests by BamHI and NheI for which the expected bands are 3.4 kb (the vector) and 0.8 kb (GFP). The 0.8 kb band is not visible on this gel. A combination of λ DNA-HindIII and φX174 DNA-HaeIII was used as ladder.

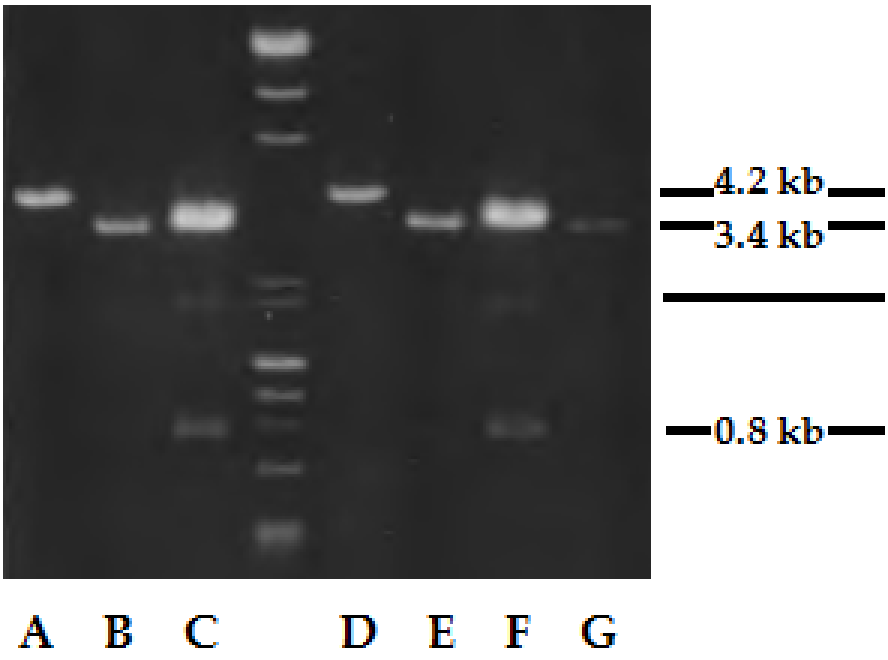

Figure 3.4 Confirmation of pTRE3G-SΔS-GFP

The gel shows multiple digest products of 2 separate plasmid extractions. Lanes A and D are single digests by NheI which recognizes only one restriction site on the expected plasmid. Lanes B and E are digests by NheI and SalI for which the expected bands are 3.4 kb (the vector) and 0.8 kb (GFP, not visible). Lanes C and F are the same double digest with increased mass showing the smaller band. There is an additional unknown band assumed to be uncut plasmid. Lane G contains plasmid pTRE3G digested with SalI. A combination of λ DNA-HindIII and φX174 DNA-HaeIII was used as ladder.

extraction. The presence of the correct plasmid construction was confirmed by digesting with SalI in search of the 4.2 kb vector-GFP fragment and the 2.4 kb lamin A gene (Fig 3.5). However, it was also necessary to test each of the extractions by diagnostic PCR, once with primers AW-136 and AW-137 (the forward insert), and once with AW-136 and AW-138 (the reverse insert, Fig 2.11). Samples displaying the correct band pattern after electrophoresis (Fig 3.6) are from plasmid pTRE3G-SΔS-GFP-laminA (Fig 3.1 E).

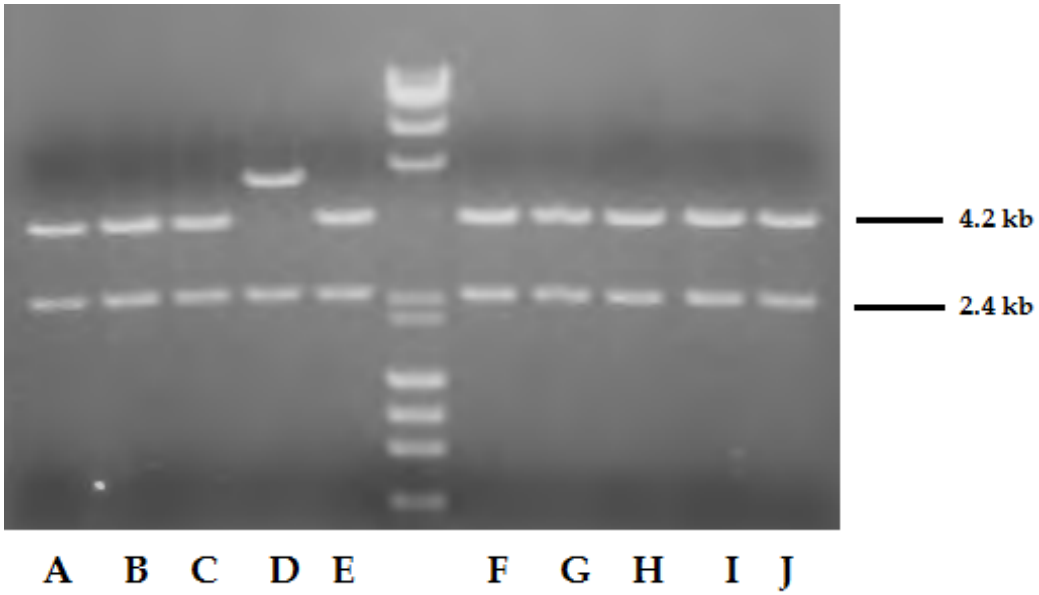

Figure 3.5 SalI Digest of Potential pTRE3G-SΔS-GFP-laminA Extracts

Lanes A-C and F-J show the smaller lamin A band and the larger vector-GFP band. Lane D shows an unknown band and was rejected. A combination of λ DNA-HindIII and φX174 DNA-HaeIII was used as ladder.

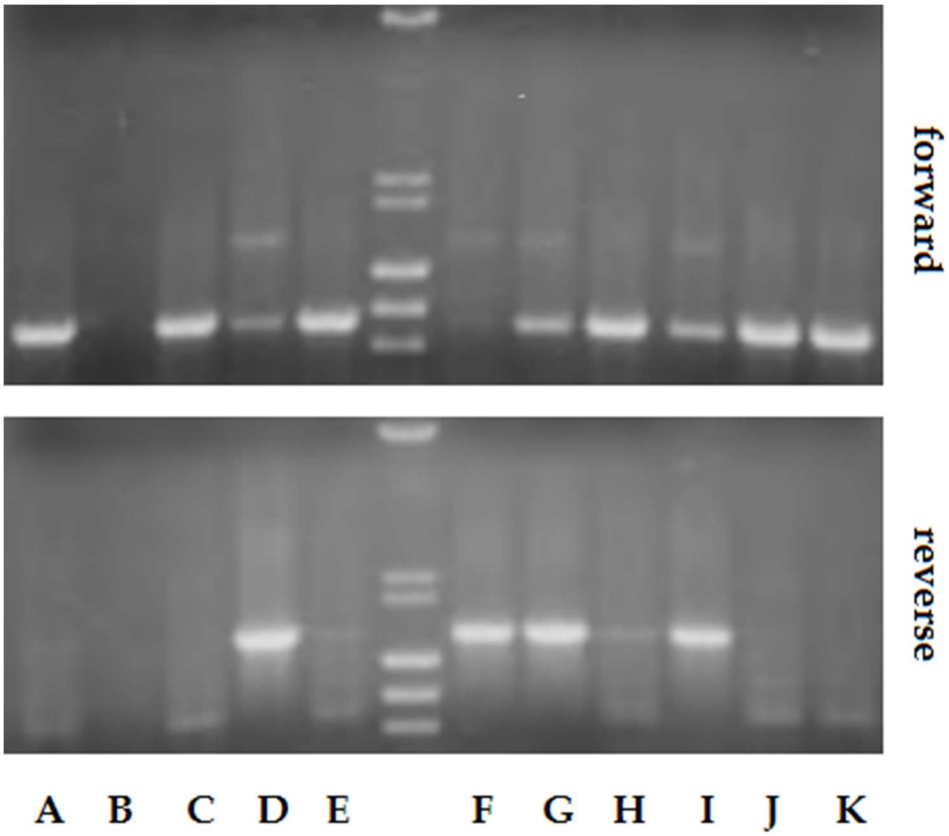

Figure 3.6 Forward and Reverse Inserts of lamin A into pTRE3G-SΔS-GFP

The figure shows PCR products for primers AW-136/137 (forward product, top), and AW-136/138 (reverse product, bottom). See Fig 2.11 for details. Lane A contains pBABE-puro-GFP-laminA, positive control for the forward product. Lane B is a negative control containing no starting DNA. Lanes D, F, G, and I contain amplification products from cells with the reverse insert plasmid. Lanes C, J, and K contain products from cells with the forward insert also confirmed not to bear the reverse insert plasmid. The samples in lanes C and K were kept as representative samples of plasmid pTRE3G- SΔS-GFP-laminA. Lanes E and H are ambiguous and were rejected for use. A combination of λ DNA-HindIII and φX174 DNA-HaeIII was used as ladder.

Chapter 4: Effect of Progerin on DSB Repair

Identification of GFP-progerin in HGPS cells and cells modeling HGPS

In previous studies, a single copy of plasmid pLB4 was stably integrated into human fibroblasts of cell line GM637 (Wang et al. 2011). Cultures of this cell line—pLB4/11—were transfected with either pBABE-puro-GFP (Fig 2.5) or pBABE-puro-GFP-progerin (Fig 2.4) by electroporation. After allowing a suitable period to recover, cells were cultured for selection in media containing puromycin. Electroporation efficiency was 4.33 colonies per million cells for plasmid pBABE-puro-GFP and 4.85 per million for plasmid pBABE-puro-GFP-progerin (Table 4.1). Several surviving colonies were cultured and screened for GFP expression (Figs 4.1 and 4.2). For cultures with strong fluorescence, protein was extracted to determine the level of expression by Western blot. Samples were probed with anti-GFP (Fig 4.3) and anti-progerin (Fig 4.4) antibodies in search of GFP and fusion protein GFP-progerin (27 and 95 kDa respectively). Anti-GFP consistently assayed with darker bands than anti-progerin. Samples pBABE-puro-GFP-progerin-21, pBABE-puro-GFP-progerin-13, and pBABE-puro-GFP-6C were chosen for exceptional GFP activity relative to other cell lines.

Table 4.1 Colonies Recovered from pLB4/11 Cells after Transfection with pBABE Derivatives

Transfected Plasmid	Cells Plated (10^6)	Colonies	Colonies/cell (10^{-6})
pBABE-puro-GFP	15	65	4.33
pBABE-puro-GFP-progerin	20	97	4.85

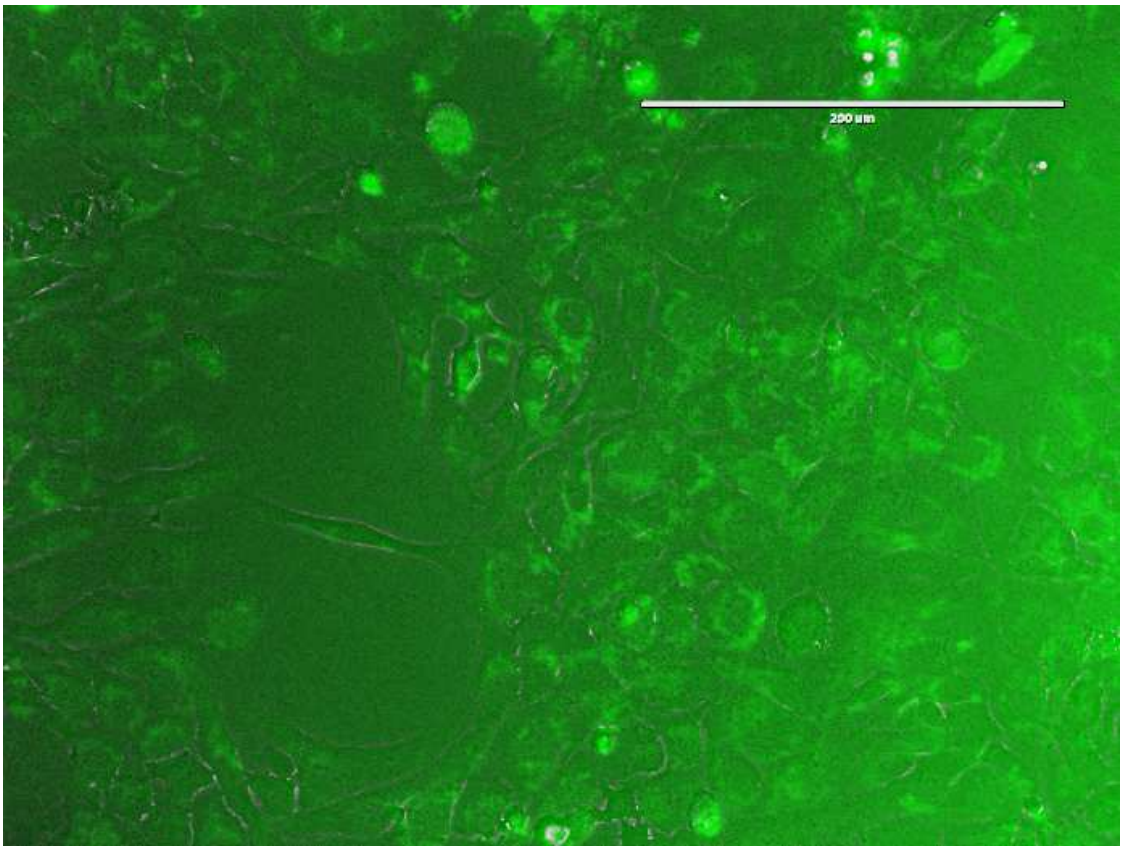

Figure 4.1 Microscopy Image of pBABE-puro-GFP-6C

GFP fluorescence image of cells expressing GFP.

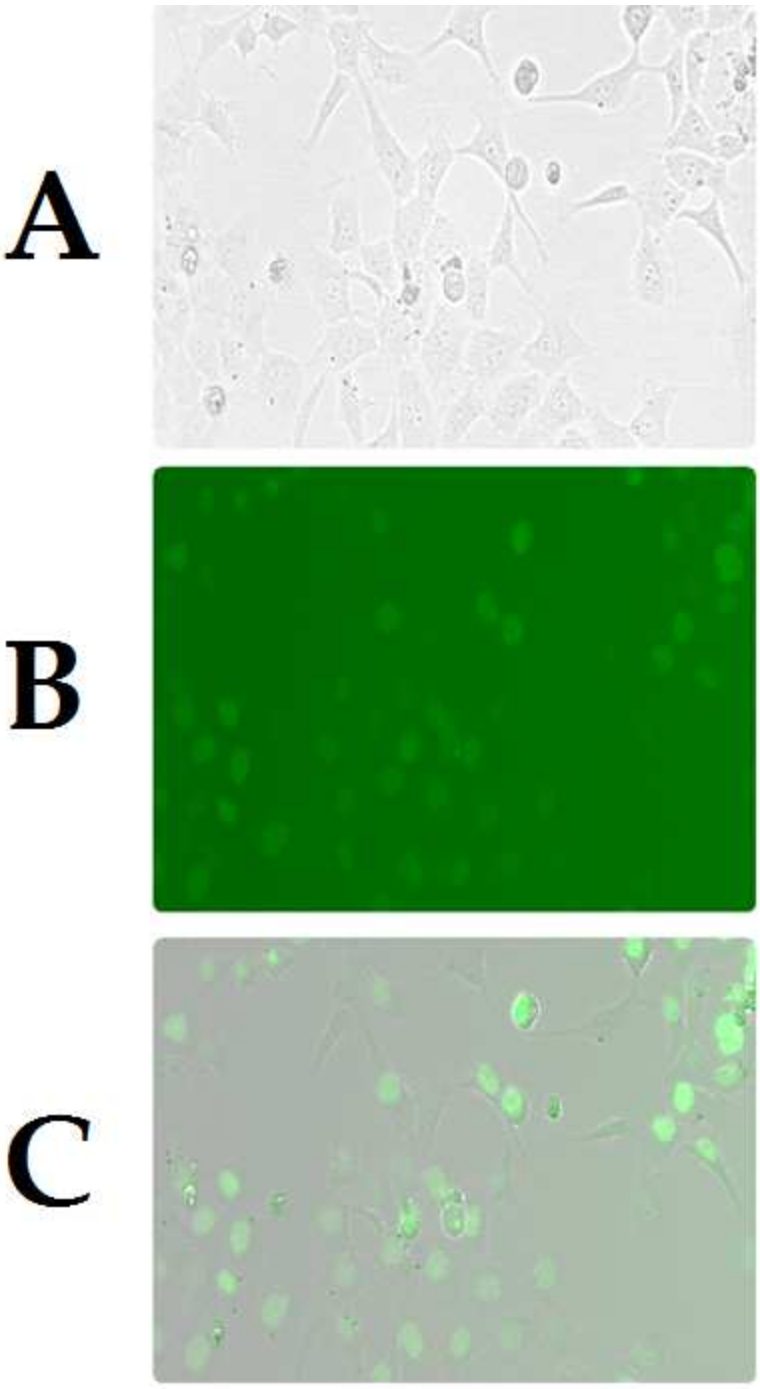

Figure 4.2 Microscopy Images of pBABE-puro-GFP-progerin-21

Visible light (A), GFP florescence (B), and overlay (C) images of cells expressing GFP-progerin. Note nuclear localization of GFP.

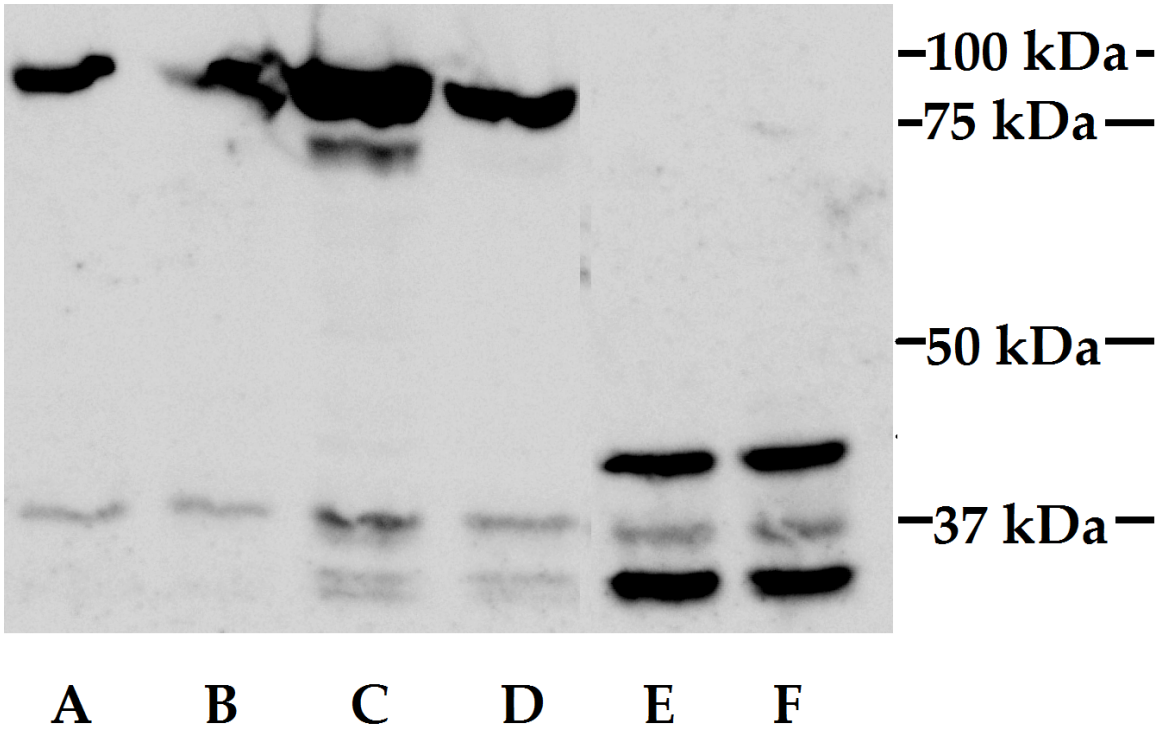

Figure 4.3 Western Blot Confirming Expression of GFP

Protein was extracted from cell lines stably integrated with pBABE-puro-GFP or pBABE-puro-GFP-progerin. These extracts were assayed by western blot using an anti-GFP antibody. Lanes A-D contain extracts from pBABE-puro-GFP-progerin cell lines 5, 18, 21, and 22 respectively. Lanes E and F contain extracts from pBABE-puro-GFP cell lines 3A and 6C respectively.

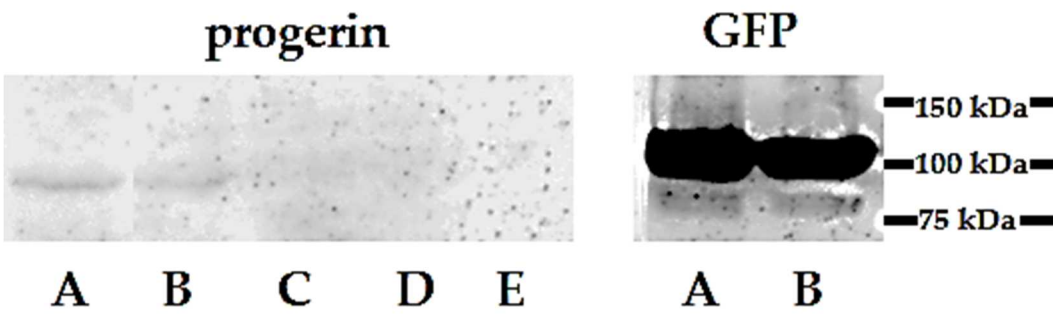

Figure 4.4 Western Blots Confirming Expression of the GFP-progerin Fusion Protein

Protein was extracted from cell lines stably integrated with pBABE-puro-GFP-progerin. These extracts were assayed on western blots using either an anti-progerin or an anti-GFP antibody. Lanes A-E contain extracts from pBABE-puro-GFP-progerin cell lines 21, 13, 5, and 1, respectively.

To provide context for these results, HGPS and unaffected cell lines were acquired from the Progeria Research Foundation. Protein extracts from cell lines HGMDFN370 (HGPS patient) and HGMDFN371 (unaffected parent of HGMDFN370) were compared to cell lines expressing GFP and GFP-progerin cell lines by Western blot using anti-lamin A primary antibody. Anti-lamin A reacted to all samples, yielding two bands as expected of lamin A (70 kDa) and lamin C (60 kDa) (Fisher, et al. 1986) (Fig 4.5 and 4.6). Anti-progerin blots were also used to compare the level of expression of GFP-progerin to the progerin expression found in HGPS cells. However, anti-progerin did not unambiguously identify the expected 68 kDa band for native progerin in HGMDFN370 (or any other sample) despite reacting with GFP-progerin (Fig 4.6). Furthermore, the polyclonal anti-lamin A did not identify native progerin nor GFP-progerin (Fig 4.5).

Analysis of DSB repair in cells expressing GFP-progerin

Subsequently, pBABE-puro-GFP-progerin cells were transiently transfected with pSce to induce a break within the tk/neo gene on pLB4. This was performed for two replicates of pBABE-puro-GFP-6C as well as two replicates of pBABE-puro-GFP-progerin-13 and four replicates of pBABE-puro-GFP-progerin-21. These replicates were cultured in media with G418 to select for functional repair of the tk/neo fusion gene. The two GFP-progerin replicates had

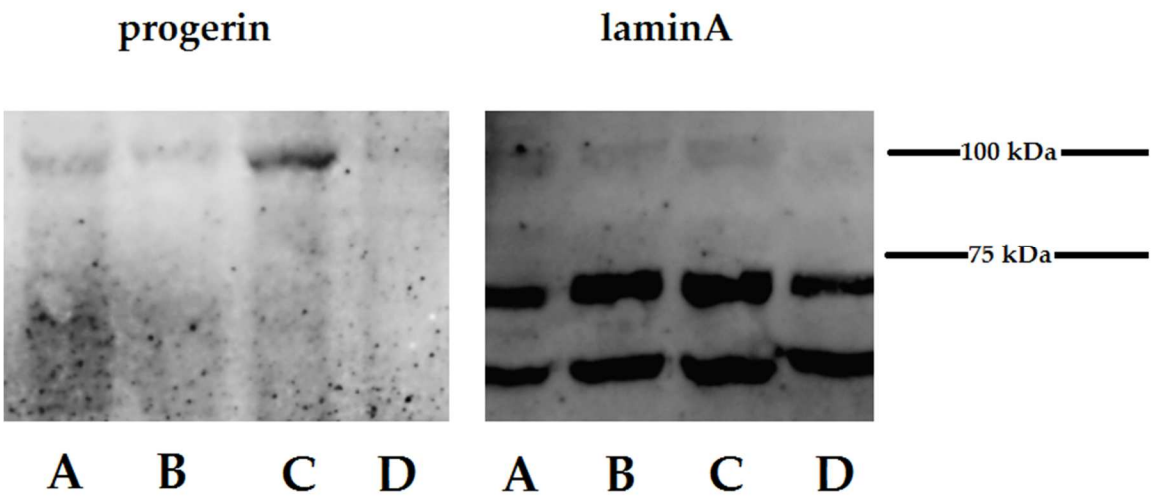

Figure 4.5 Western Blots Confirming Expression of Progerin and LaminA

Protein was extracted from cell lines stably integrated with pBABE-puro-GFP or pBABE-puro-GFP-progerin and from the parent cell line pLB4/11. These extracts were assayed on western blots using either an anti-progerin or an anti-laminA antibody. Lane A contains extract from pLB4/11. Lanes B and C contain extracts from pBABE-puro-GFP-progerin cell lines 5 and 21, respectively. Lane D contains extract from pBABE-puro-GFP cell line 6C.

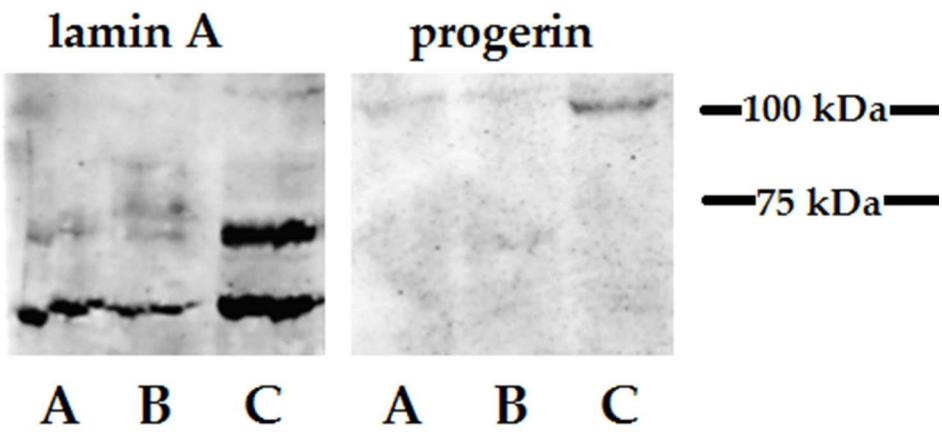

Figure 4.6 Western Blots Comparing expression of Progerin and LaminA between HGPS and GFP-progerin Expressing Cell Lines

Protein extracts from HGMDFN371 (lane A), HGADFN370 (lane B) and cell line pBABE-puro-GFP-progerin-21 (lane C) were assayed by western blot using an anti-laminA or an anti-progerin antibody. HGADFN370 is a HGPS patient, and HGMDFN371 is an unaffected parent of HGADFN370.

rates of survival of 26.4 and 21.0 colonies per 10^4 cells; GFP colonies survived at a rate of 7.11 per 10^4 (Table 4.2). Representatives of surviving colonies were recovered and cultured. DNA was extracted from these cells and amplified by PCR with primers AW-85 and AW-91 (Fig 2.12). Approximately 31% (11) of GFP-expressing colonies and 25% (15) of those expressing GFP-progerin did not yield an amplification product despite surviving selection (Table 4.3). A further 5% of GFP-progerin colonies yielded product of an unexpected size. Successfully amplified products were sequenced to determine the method of repair. Sequencing data was interpreted by sequence alignment using the tk recipient and donor as standards (Fig 2.13). NHEJ events are characterized by insertions/deletions which leave the recipient markers intact. GC events replace a number of the recipient markers with donor but do not affect the flanking regions of the recipient. A third class of events, homology dependent deletion (HDD), includes both single-strand annealing and crossover, since these two are indistinguishable within this substrate. HDD events are fusions of the donor and recipient tk genes and are characterized by a track of markers that ends downstream of the I-SceI site and extends upstream beyond the sequencing window. To distinguish between homology dependent deletions and long gene conversions which extend beyond the first marker, genomic DNA was also subjected to Southern blotting analysis. The genomic DNA was digested with

Table 4.2 Colonies Recovered from pBABE Transfected Cell Lines after Induced DSB and Selection in G418

Cell Line	Electroporation	Cells Plated (10^4)	Colonies	Colonies/cell (10^{-4})	Mean Colonies/cell by cell line (10^{-4})
pBABE-puro-GFP-progerin-21	A	5.0	195	39.0	26.4
	B	5.0	121	24.2	
	C	4.0	145	36.3	
	D	5.0	31	6.2	
pBABE-puro-GFP-progerin-13	A	5.0	102	20.4	21.0
	B	5.0	108	21.6	
pBABE-puro-GFP-6C	1	50	310	6.2	7.11
	2	50	401	8.0	

Table 4.3 Products Recovered from G418 Resistant Cells with a Stably Integrated Variant of Plasmid pBABE-puro

pBABE derivative	Expected	None	Irregular
GFP-6C	24	11	0
GFP-progerin-13	9	7	3
GFP-progerin-21	33	8	0

Amplification products are those resulting from primers AW-85 and AW-91. Irregular results are those samples displaying a band which differs significantly in size from the control.

HindIII and XbaI and then blotted with ^{32}P-labeled probe for the tk gene. HDD events may be distinguished from gene conversions by the differing banding pattern (Fig 2.1 and 4.7). Blotting patterns confirmed the preliminary results of sequencing in nearly all (97%) samples.

A total of 68 GFP-progerin expressing cultures and 36 GFP expressing cultures were analyzed. NHEJ events were identified by the lack of donor markers in the sequencing window (Fig 4.8). GC events were identified by donor markers flanked by recipient markers (Fig 4.9). HDD events were identified by donor markers extending upstream to the limit of the sequencing window (Fig 4.10). In cells expressing GFP-progerin, analysis indicates that approximately 30% of events that yielded PCR products were GC, 36% were HDD, and 34% were NHEJ (Table 4.4). It should be noted that only repair events which restore the reading frame will survive selection; therefore, the rate of NHEJ is (presumably) three times the observed value. GFP expressing cells displayed repair events of 20% GC, 76% HDD, and 4% NHEJ, a drastically lower incidence of NHEJ compared to GFP-progerin expressing cells ($p = 4.70 \times 10^{-3}$ by Pearson's chi-squared test, Table 4.4). However, both the GFP and GFP-progerin expressing cell cultures included events that did not yield PCR products, 31% and 26% of total events, respectively. No such events were found in pLB4/11 ($p = 2.20 \times 10^{-7}$, Table 4.4). A

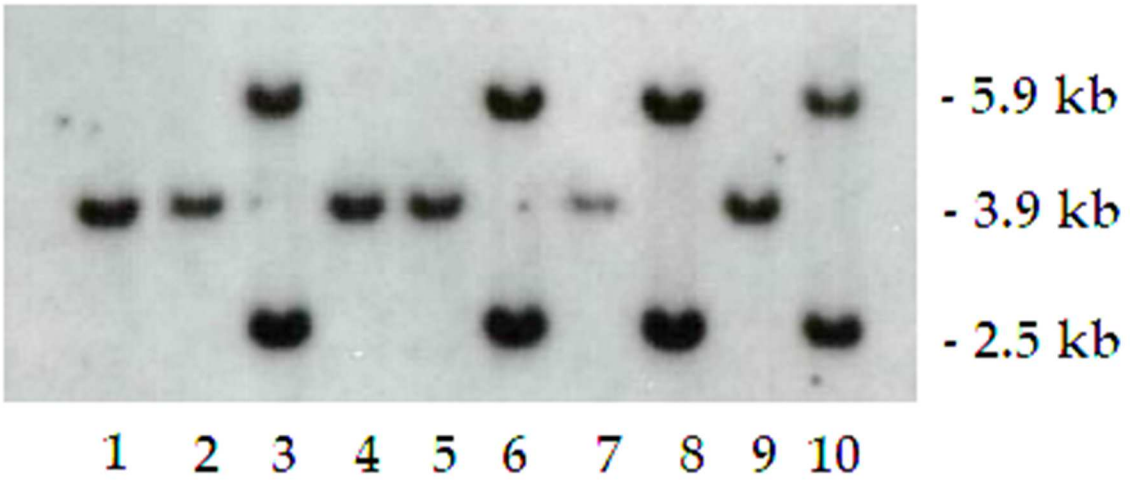

Figure 4.7 Example Southern Blot of Digest Products of the pLB4 Recombination Substrate

As described in Figure 2.1, the repaired pLB4 recombination substrate displays two different banding patterns after HindIII/XbaI digest depending upon method of repair. Samples for which sequencing could not distinguish between HDD and GC events were digested and assayed by Southern blot alongside additional known events. Lanes 1, 2, 4, 5, 7, and 9 show the single band characteristic of HDD. Lanes 3, 6, 8, and 10 show the two bands characteristic of GC. It is not necessary to assay NHEJ samples because they can be unambiguously identified through sequencing. All samples shown are derived from cell line pBABE-puro-GFP-6C (sub-clones 7D, 8C, 8D, 9A, 9B, 9C, 9D, 9E, 10C, 10E).

Sample	Repair Site	Deletion (bp)
Recipient	tggg[agcttagggata--acagggtaat]agctca	N/A
21-A-2	tggg[agcttaggga----------]----ca	16
21-A-4	tgg-[----------acagggtaat]agctca	13
21-A-9	tggg[agcttagggata---------aat]agctca	7
21-B-1	tggg[agcttagggata---cagggtaat]agctca	1
21-B-24	tggg[agctta-----------ggtaat]agctca	10
21-C-3	tggg[agctta-----------ggtaat]agctca	10
21-C-5	tggg[agcttagggata---cagggtaat]agctca	1
21-C-8	tggg[agcttagg---------gggtaat]agctca	7
21-C-15	tggg[agcttagggata---cagggtaat]agctca	1
21-C-18	tggg[agctt----------]-----a	22
21-D-3	tggg[agcttagg-------c--ggtaat]agctca	7
21-D-21	tggg[agctta-----------ggtaat]agctca	10
13-A-2	----[----------]------	151
13-B-1	----[----------]------	79
13-B-4	----[----------]------	1126
2A (GFP)	tggg[agcttagggatattacagggtaat]agctca	+2 (insertion)

Figure 4.8 G418^R Clones that Yielded NHEJ Events.

Brackets show the location of the I-SceI insert. The red "c" base shows the location of homeologous marker #5. NHEJ repairs must result in a -1 frame shift in order to restore function to *neo*. All NHEJ events in induced DSB clones from GFP-progerin cell line 13 resulted in very large (≥ 79 bp) deletions, in contrast to the more modest (≤ 22 bp) events from cell line 21. Clones expressing GFP resulted in only 1 NHEJ event among them. Clones from the fluctuation test did not yield identifiable NHEJ events.

Recipient	G	C	G	A	v	C	G	T	A	T	C	T	T	A
Donor	C	A	T	G		T	T	C	G	G	T	C	C	C
GFP														
8D	*	C	G	G		T	T	C	G	G	*	*	*	*
9C	*	C	G	G		T	T	C	G	T	*	*	*	*
9E	*	C	G	G		T	G	T	A	T	*	*	*	*
10D	*	C	G	G		T	G	T	*	*	*	*	*	*
10E	*	C	G	G		T	G	T	A	T	*	*	*	*
GFP-progerin														
13-A-4	*	C	G	G		T	*	*	*	*	*	*	*	*
13-B-13	*	C	G	G		T	T	C	G	G	*	*	*	*
13-B-16	*	C	G	G		T	G	T	A	T	*	*	*	*
13-B-23	*	C	G	G		T	G	T	A	T	*	*	*	*
21-A-1	G	C	G	G		T	G	T	A	T	C	T	T	A
21-A-3	G	C	G	G		T	G	T	A	T	C	T	T	*
21-B-21	G	C	G	G		T	G	T	A	T	C	T	T	A
21-C-1	*	C	G	G		T	G	T	A	T	*	*	*	*
21-C-2	*	C	G	A		T	G	T	A	T	*	*	*	*
21-C-6	*	C	G	A		T	G	T	A	T	*	*	*	*
21-C-12	*	*	G	A		T	G	T	A	T	*	*	*	*
21-C-19	*	C	G	G		T	T	C	G	T	*	*	*	*
21-D-6	*	C	G	A		T	G	T	A	T	*	*	*	*
21-D-17	*	C	G	G		T	G	T	A	T	*	*	*	*
21-D-22	*	C	G	G		T	T	C	A	T	*	*	*	*
GFP-progerin (fluctuation)														
13-4-γ	G	C	G	G		T	G	T	A	T	C	*	*	*
13-4-δ	*	C	G	G		T	G	T	A	T	C	*	*	*
13-4-ζ	G	C	G	G		T	G	T	A	T	C	*	*	*
13-7-δ	G	C	G	G		T	G	T	A	*	*	*	*	*

Figure 4.9 G418^R Clones that Yielded Gene Conversion Events

G418^R clones were sequenced and compared to the donor and recipient tk genes. Clones listed in the figure included repair events in which a portion of the recipient bases were replaced by donor bases. The yellow highlight indicates donor mismatches found within the repaired sequences. Asterisks indicate insufficient or ambiguous data. The caret in the recipient sequence marks the location of the I-SceI recognition site.

Recipient	G	C	G	A	v	C	G	T	A	T	C	T	T	A
Donor	C	A	T	G		T	T	C	G	G	T	C	C	C
GFP														
1B	*	A	T	G		T	G	T	A	T	*	*	*	*
1E	*	A	T	G		T	T	C	G	G	*	*	*	*
2E	*	A	T	G		T	G	T	A	T	*	*	*	*
4B	*	A	T	G		T	T	C	G	*	*	*	*	*
4C	*	A	T	G		T	T	C	G	G	*	*	*	*
4E	*	A	T	G		T	T	C	G	G	*	*	*	*
5C	*	A	T	G		T	T	C	G	G	*	*	*	*
5D	*	A	T	G		T	T	C	G	G	*	*	*	*
6B	*	A	T	G		T	G	T	A	T	*	*	*	*
6C	*	A	T	G		T	T	C	G	C	*	*	*	*
6E	*	A	T	G		T	T	C	G	*	*	*	*	*
7D	*	A	T	G		T	T	C	G	*	*	*	*	*
8A	*	A	T	G		T	T	C	G	G	*	*	*	*
8C	*	A	T	G		T	G	T	A	T	*	*	*	*
9A	*	A	T	G		T	G	T	A	T	*	*	*	*
9B	*	A	T	G		T	T	C	G	G	*	*	*	*
9D	*	A	T	G		T	T	C	G	G	*	*	*	*
10C	*	A	T	G		T	T	C	G	G	*	*	*	*
GFP-progerin														
13-A-3	*	*	T	G		T	T	C	G	G	*	*	*	*
13-A-12	*	A	T	G		T	*	*	*	*	*	*	*	*
13-A-17	*	A	T	G		T	T	C	*	*	*	*	*	*
13-B-14	*	A	T	G		T	T	C	G	G	*	*	*	*
21-B-23	*	A	T	G		T	T	C	G	G	T	?	?	?
21-C-7	*	A	T	G		T	T	C	G	G	*	*	*	*
21-C-14	*	A	T	G		T	G	T	A	T	*	*	*	*
21-C-16	*	A	T	G		T	G	T	A	T	*	*	*	*
21-C-20	*	A	T	G		T	T	C	G	C	*	*	*	*
21-C-21	*	A	T	G		T	T	C	G	G	*	*	*	*
21-C-23	*	A	T	G		T	G	T	A	T	*	*	*	*
21-D-4	*	A	T	G		T	G	T	A	T	*	*	*	*
21-D-11	*	A	T	G		T	G	T	A	T	*	*	*	*
21-D-13	*	A	T	G		T	T	C	G	G	*	*	*	*
21-D-14	*	A	T	G		T	T	C	G	G	*	*	*	*
21-D-15	*	A	T	G		T	T	C	G	*	*	*	*	*
21-D-16	*	A	T	G		T	T	C	G	G	*	*	*	*
21-D-18	*	A	T	G		T	T	C	G	G	*	*	*	*
GFP-progerin (fluctuation)														
13-2-ι	*	A	T	G		T	T	C	G	G	T	*	*	*
13-7-θ	C	A	T	G		T	T	C	G	G	T	*	*	*
13-2-κ	C	A	T	G		T	T	C	G	G	T	*	*	*

Figure 4.10 G418^R Clones that Yielded Homology Dependent Deletion Events

G418^R clones were sequenced and compared to the donor and recipient tk genes. Clones listed in the figure included repair events in which the recipient sequence was joined to the donor. The yellow highlight indicates donor mismatches found within the repaired sequences. Asterisks indicate insufficient or ambiguous data. The caret in the recipient sequence marks the location of the I-SceI recognition site.

Table 4.4 DSB Repair Events Recovered from G418 Resistant Cells with a Stably Integrated Variant of Plasmid pBABE-puro

pBABE derivative	GC	HDD	NHEJ	Unknown	Total
GFP-6C	5	19	1	11	36
GFP-progerin-13	4	5	3	7	19
GFP-progerin-21	12	14	15	8	49
none	32	22	23	0	77

Data for cells with no pBABE derivative were retrieved from Wang et al. 2011.

small number of these events present unusual banding patterns on Southern blots (Fig 4.11), though the significance of this finding is not clear.

Spontaneous repair events in cells expressing GFP-progerin

Additional pBABE-puro-GFP-progerin-13 cells were subjected to a fluctuation test to recover spontaneous HR events, again in G418. Survival ranged from 1.1 cells per 10^4 to less than 5.0 per 10^7 (Table 4.5). Genomic DNA extracted from the resulting colonies was also subjected to PCR and sequencing. All of the samples from fluctuation cultures yielded product for primers AW-85 and AW-91. Sequencing revealed that 33% of repair events were GC, 28% HDD, and 39% could not be identified because no deviation from the recipient sequence could be found within the sequencing window (Table 4.6).

Discussion

This experiment was conducted for the purpose of studying the effect of constitutive progerin expression on DSB repair. The presence of GFP-progerin in cells significantly increased the rate of GC and NHEJ relative to HDD when compared to rates of those events in GFP-expressing cells. The largest rate increase is in NHEJ, indicating that the cell is forced to rely upon NHEJ more often than upon HR despite the superior fidelity of the latter (Fig 4.12). This links progerin—and, by extension, natural aging—to the fidelity of break repair mechanisms and lends credence to the idea of aging as a disease of DSB repair.

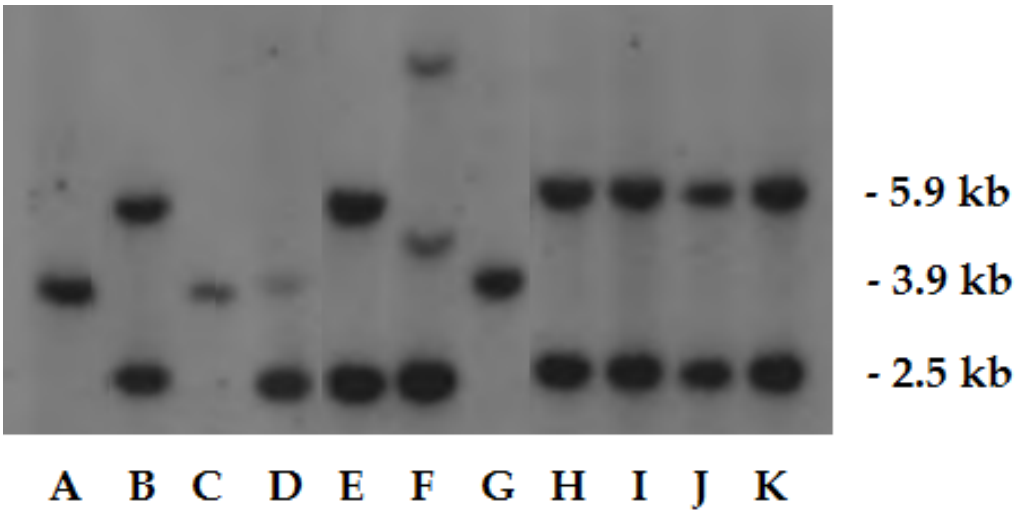

Figure 4.11 Example Southern Blot of G418^R Clones that did not Yield Amplification Product after PCR with Primers AW-85 and AW-91

Several colonies which survived selection did not yield a product suitable for sequencing. Lanes A-E contain DNA from sub-clones derived from pBABE-puro-GFP-6C (in order: 2A, 3A, 3C, 6D, and 7A). Lanes F-I contain DNA from sub-clones derived from pBABE-puro-GFP-progerin-21 (in order: 21-B-16, 21-C-4, 21-C-10, 21-D-1, and 21-D-12). Lane J contains DNA from sub-clone pBABE-puro-GFP-progerin-13-B-12. None of the aforementioned samples yield amplification product. Lane K contains DNA from cell line pBABE-puro-GFP-progerin-13 before induced break and selection. Note lanes D and F which do not present either of the expected banding patterns.

Table 4.5 Colonies Recovered from Fluctuation Test of pBABE-puro-GFP-progerin-13

Sub-Clone	Cells Plated (10^6)	Colonies	Colonies/cell (10^{-7})
2	10	1132	113
4	10	20	2.00
5	2.0	1	0.50
6	3.0	0	0.00
7	7.0	6	0.86
9	5.0	0	0.00

Cells were selected in G418. No break was induced before selection. Additional sub-clones were discarded due to contamination.

Table 4.6 Repair Events Recovered from G418 Resistant Cells after Fluctuation Test

Sub-Clone	GC	HDD	Unknown	Total
2	0	1	7	8
4	5	1	0	6
7	1	3	0	4

Cells were selected in G418. No break was induced before selection.

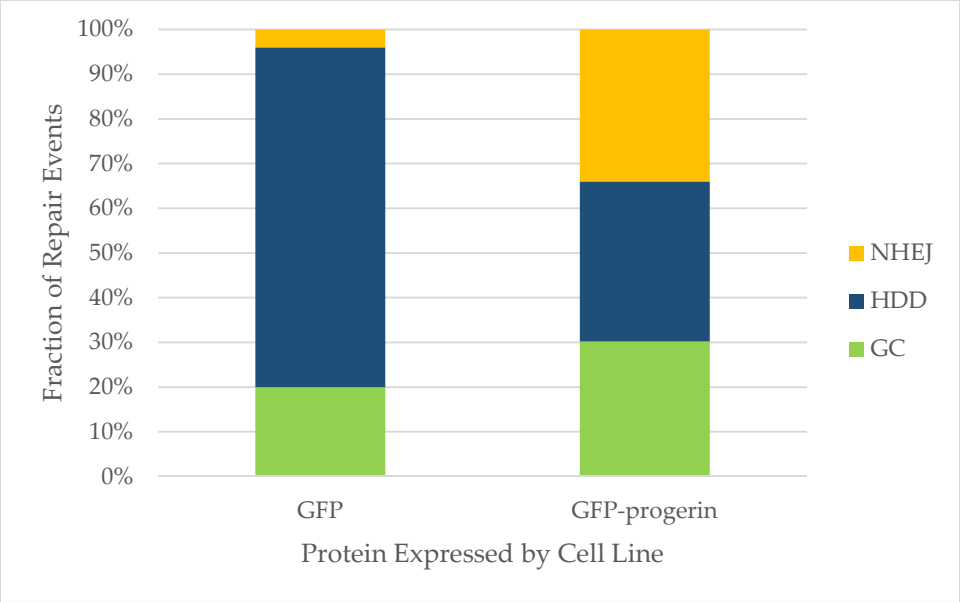

Figure 4.12 Ratio of DSB Repair Events in Cells According to Protein Expressed

Plasmid pBABE-puro-GFP served as a control to be tested in parallel to plasmid pBABE-puro-GFP-progerin. However, it was discovered that cells expressing GFP displayed a class of repair events not found in the parent cell line pLB4/11 as reported in previous studies (Fig 4.13). A possible explanation for this discrepancy can be found in the scientific literature (Wallace et al. 2013). Green fluorescent protein has been linked to inflammation (Mak et al. 2007), neuropathy (Krestel et al. 2004), and apoptosis (Liu et al. 1999). The mechanism of toxicity has not been fully explained, nor does it appear that any correlation has been confirmed or rejected relative to DNA repair. There remains a possibility that free GFP has different cellular activity than GFP appended to a fusion protein (regardless of the identity of the fusion). In future studies, cells integrated with pBABE-puro-GFP-laminA would serve as a useful control to compare against pBABE-puro-GFP-progerin by showing the difference between elevated expression of functional laminA to elevated D50-laminA (progerin). The empty vector (pBABE-puro) may also serve as a control.

Concerning the forms of repair detectable by the methods employed—gene conversion, homology-dependent deletion, non-homologous end joining—cells expressing GFP-progerin were not significantly different from pLB4/11 cells. However, both GFP and GFP-progerin expressing cell cultures yielded repair events that could not be characterized by the assays used. These uncharacterized

results fail to yield a PCR product using primers AW-85 and AW-91, and two of these events display unusual banding patterns on Southern blots (Fig 4.11). Such results have not been found in the parent cell line (Table 4.4, Fig 4.13).

Spontaneous repair also included uncharacterized events. However, despite the failure to fully characterize them, they are demonstrably distinct: all of these spontaneous events yielded PCR product in contrast to none of the uncharacterized break-induced events. Furthermore, all of these spontaneous events are derived from the same sub-clone of the fluctuation test, so they may be descendants of a single repair event. Without additional research to explicitly identify the repair events, statistical tests of these spontaneous/induced results are of only marginal value.

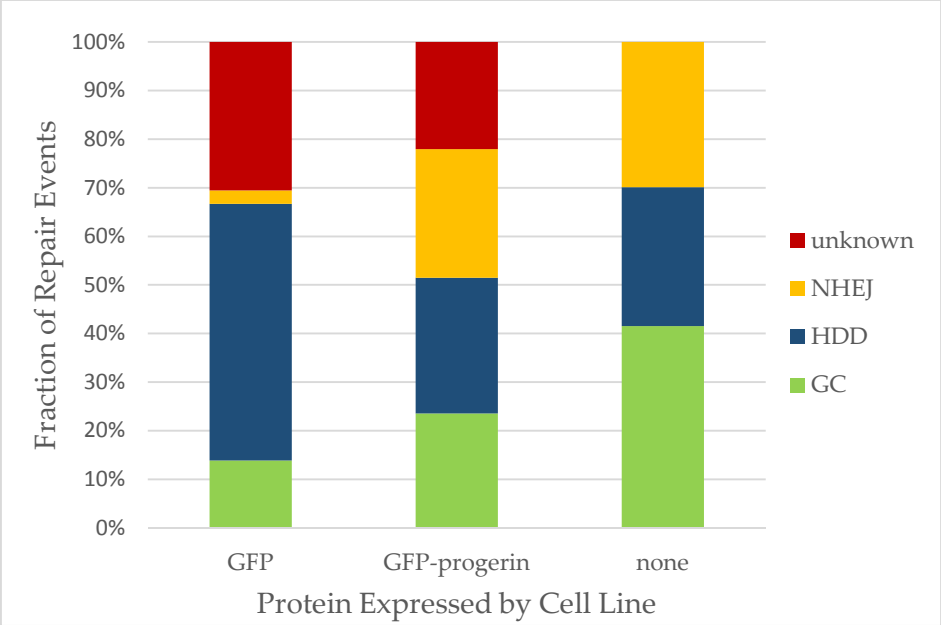

Figure 4.13 Expanded Data on Ratio of DSB Repair Events in Cells According to Protein Expressed

References

Ackerman, J., E. Gilbert-Barness. 2002. Hutchinson-Gilford Progeria Syndrome: a Pathologic Study. *Pediatric Pathology and Molecular Medicine* 21: 1-13.

Baumann, P., S. C. West. 1998. Role of the human RAD51 protein in homologous recombination and double-strand break repair. *Trends in Biochemical Sciences* 23(7): 247-251.

Bennardo, N., A. Cheng, N. Huang, J. M. Stark. 2008. Alternative-NHEJ Is a Mechanistically Distinct Pathway of Mammalian Chromosome Break Repair. *PLoS Genetics* 4(6): e1000110.

Broers, J. L. V., B. M. Machiels, G. J. J. M. van Eys, H. J. H. Kuijpers, E. M. M. Manders, R. van Driel, F. C. S. Ramaekers. 1999. Dynamics of the nuclear lamina as monitored by GFP-tagged A-type lamins. *Journal of Cell Science* 112: 3463-3475.

Burke, B., C. L. Stewart. 2002. Life at the edge: the nuclear envelope and human disease. *Nature Reviews. Molecular Cell Biology* 3(8): 575-585.

Cao, K., B. C. Capell, M. R. Erdos, K. Djabali, F. S. Collins. 2007. A lamin A protein isoform overexpressed in Hutchinson–Gilford progeria syndrome interferes with mitosis in progeria and normal cells. *Proceedings of the National Academy of Sciences of the United States of America* 104(12): 4949-4954.

Cha, R. S., N. Kleckner. 2002. ATR Homolog Mec1 Promotes Fork Progression, Thus Averting Breaks in Replication Slow Zones. *Science* 297: 602-606.

Collins, S., H. Coleman, M. Groudine. 1987. Expression of bcr and bcr-abl Fusion Transcripts in Normal and Leukemic Cells. *Molecular and Cellular Biology* 7(8): 2870-2876.

Constantinescu, D., A. B. Csoka, C. S. Navara, G. P. Schatten. 2010. Defective DSB repair correlates with abnormal nuclear morphology and is improved with FTI treatment in Hutchinson-Gilford progeria syndrome fibroblasts. *Experimental Cell Research* 316: 2747-2759.

Corso, C., E. M. Parry, R. G. A. Faragher, A. Seager, M. H. L. Green, J. M. Parry. 2005. Molecular cytogenetic insights into the ageing syndrome Hutchinson-Gilford Progeria (HGPS). *Cytogenetic and Genome Research* 111: 27-33.

Domínguez-Gerpe, L., D. Araújo-Vilar. 2008. Prematurely aged children: molecular alterations leading to Hutchinson-Gilford progeria and Werner syndromes. *Current Aging Science* 1(3): 202-212.

Eriksson, M., W. T. Brown, L. B. Gordon, M. W. Glynn, J. Singer, L. Scott, M. R. Erdos, C. M. Robbins, T. Y. Moses, P. Berglund, A. Dutra, E. Pak, S. Durkin, A. B. Csoka, M. Boehnke, T. W. Glover, F. S. Collins. 2003. Recurrent de novo point mutations in lamin A cause Hutchingson-Gilford progeria syndrome. *Nature* 423: 293-298.

Fisher, D. Z., N. Chaudhary, G. Blobel. 1986. cDNA sequencing of nuclear lamins A and C reveals primary and secondary structural homology to intermediate filament proteins. *Proceedings of the National Academy of Sciences of the United States of America* 83(17): 6450-6454.

Gorbunova, V., A. Seluanov. 2005. Making ends meet in old age: DSB repair and aging. *Mechanisms of ageing and development* 126: 621-628.

Glynn, M. W., T. W. Glover. 2005. Incomplete processing of mutant lamin A in Hutchinson-Gilford progeria leads to nuclear abnormalities, which are reversed by farnesyltransferase inhibition. *Human Molecular Genetics* 14(20): 2959-2969.

Helleday, T. 2003. Pathways for mitotic homologous recombination in mammalian cells. *Mutation Researh-Fundamental and Molecular Mechanisms of Mutagenesis* 532(1-2): 103-115.

Hutchinson, J. 1886. Congenital Absence of Hair and Mammary Glands with Atrophic Condition of the Skin and its Appendages in a Boy whose

Mother had been almost wholly Bald from Alopecia Areata from the age of Six. *Medico-Chirurgical Transactions* 69: 473-477.

Jackson, S. P. 2002. Sensing and repairing DNA double-strand breaks. *Carcinogenesis* 23(5): 687-696.

Kelley, J. B., S. Datta, C. J. Snow, M. Chatterjee, L. Ni, A. Spencer, C. Yang, C. Cubeñas-Potts, M. J. Matunis, B. M. Paschal. 2011. The Defective Nuclear Lamina in Hutchinson-Gilford Progeria Syndrome Disrupts the Nucleocytoplasmic Ran Gradient and Inhibits Nuclear Localization of Ubc9. *Molecular and Cellular Biology* 31(16): 3378-3395.

Kim, P. M., C. Allen, B. M. Wagener, Z. Shen, J. A. Nickoloff. 2001. Overexpression of human RAD51 and RAD52 reduces double-strand break-induced homologous recombination in mammalian cells. *Nucleic Acids Research* 29(21): 4352-4360.

Krestel, H. E., A. L. A. Mihaljevic, D. A. Hoffman, A. Schneider. 2004. Neuronal co-expression of EGFP and b-galactosidase in mice causes neuropathology and premature death. *Neurobiology of Disease* 17: 310-318.

Liu, H. M. Jan, C. Chou, P. Chen, N. Ke. 1999. Is Green Fluorescent Protein Toxic to the Living Cells? *Biochemical and Biophysical Research Communications* 260: 712-717.

Lukacsovich, T., D. Yang, A. S. Waldman. 1994. Repair of a specific double-strand break generated within a mammalian chromosome by yeast endonuclease I-SceI. *Nucleic Acids Research* 22(25): 5649-5657.

Lukas, J., C. Lukas, J. Bartek. 2004. Mammalian cell cycle checkpoints: signalling pathways and their organization in space and time. *DNA Repair* 3(8-9): 997-1007.

Mak, G. W., C. Wong, S. K. Tsui. 2007. Green fluorescent protein induces the secretion of inflammatory cytokine interleukin-6 in muscle cells. *Analytical Biochemistry* 362: 296-298.

McVey, M., S. E. Lee. 2008. MMEJ repair of double-strand breaks (director's cut): deleted sequences and alternative endings. *Trends in Genetics* 24(11): 529-538.

Moir, R. D., M. Yoon, S. Khuon, R. D. Goldman. 2000. Nuclear Lamins A and B1: Different Pathways of Assembly during Nuclear Envelope Formation in Living Cells. *The Journal of Cell Biology* 151(6): 1155-1168.

Morley, A. 1998. Somatic Mutation and Aging. *Annals of the New York Academy of Sciences* 854: 20-22.

O'Driscoll, M., P. A. Jeggo. 2006. The role of double-strand break repair — insights from human genetics. *Nature Reviews. Genetics* 7(1): 45-54.

Ogawa, T., X. Yu, A. Shinohara, E. H. Egelman. 1993. Similarity of the Yeast RAD51 Filament to the Bacterial RecA Filament. *Science* 259(5103): 1896-1899.

Pacheco, L. M., L. A. Gomez, J. Dias, N. M. Ziebarth, G. A. Howard, P. C. Schiller. 2014. Progerin expression disrupts critical adult stem cell functions involved in tissue repair. *Aging* 6(12): 1049-1063.

Scaffidi, P., T. Misteli. 2005. Reversal of the cellular phenotype in the premature aging disease Hutchinson-Gilford progeria syndrome. *Nature Medicine* 11(4): 440-445.

Scaffidi, P., T. Misteli. 2008. Lamin A-dependent misregulation of adult stem cells associated with accelerated ageing. *Nature Cell Biology* 10: 452-459.

Schwartz, F., N. Maeda, O. Smithies, R. Hickey, W. Edelmann, A. Skoultchi, R. Kucherlapati. 1991. A dominant positive and negative selectable gene for use in mammalian cells. *Proceedings of the National Academy of Sciences of the United States of America* 88: 10416-10420.

Smith, J. A., L. A. Bannister, V. Bhattacharjee, Y. Wang, B. C. Waldman, A. S. Waldman. 2007. Accurate Homologous Recombination Is a Prominent Double-Strand Break Repair Pathway in Mammalian Chromosomes and Is Modulated by Mismatch Repair Protein Msh2. *Molecular and Cellular Biology* 27(22): 7816-7827.

Snow, C. J., A. Dar, A. Dutta, R. H. Kehlenbach, B. M. Paschal. 2013. Defective nuclear import of Tpr in Progeria reflects the Ran sensitivity of large cargo transport. *The Journal of Cell Biology* 201(4): 541-557.

Somervaille, T. C. P., M. L. Cleary. 2010. Grist for the MLL: how do MLL oncogenic fusion proteins generate leukemia stem cells? *International Journal of Hematology* 91: 735-741.

Sonoda, E., H. Hochegger, A. Saberi, Y. Taniguchi, S. Takeda. 2006. Differential usage of non-homologous end-joining and homologous recombination in double strand break repair. *DNA Repair* 5(9-10): 1021-1029.

Stuart, G. R., B. W. Glickman. 2000. Through a Glass, Darkly: Reflections of Mutation From lacI Transgenic Mice. *Genetics* 155(3): 1359-1367.

Stiff, T., M. O'Driscoll, N. Rief, K. Iwabuchi, M. Löbrich, P. Jeggo. 2004. ATM and DNA-PK Function Redundantly to Phosphorylate H2AX after Exposure to Ionizing Radiation. *Cancer Research* 64(7): 2390-2396

Thompson, L. H., D. Schild. 2001. Homologous recombination repair of DNA ensures mammalian chromosome stability. *Mutation Research* 477(1-2): 131-153.

Uitenbroek, D. G. 1997. SISA-Binomial. <http://www.quantitativeskills.com/sisa/distributions/binomial.htm>.

Verdy, C., J. E. Branka, N. Mekideche. 2011. Quantitative assessment of lactate and progerin production in normal human cutaneous cells during normal ageing: effect of an Alaria esculenta extract. *International Journal of Cosmetic Science* 33: 462-466.

Waldman, A. S., R. M. Liskay. 1987. Differential effects of base-pair mismatch on intrachromosomal versus extrachromosomal recombination in mouse cells. *Proceedings of the National Academy of Sciences of the United States of America* 84: 5340-5344.

Waldman, A. S., R. M. Liskay. 1988. Dependence of Intrachromosomal Recombination in Mammalian Cells on Uninterrupted Homology. *Molecular and Cellular Biology* 8(12): 5350-5357.

Wallace, L. M., A. Moreo, K. R. Clark, S. Q. Harper. 2013. Dose-dependent Toxicity of Humanized Renilla reniformis GFP (hrGFP) Limits Its Utility as a Reporter Gene in Mouse Muscle. *Molecular Therapy-Nucleic Acids* 2: e86

Wang, Y., A. A. Panteleyev, D. M. Owens, K. Djabali, C. L. Stewart, H. J. Worman. 2008. Epidermal expression of the truncated prelamin A causing Hutchinson-Gilford progeria syndrome: effects on keratinocytes, hair and skin. *Human Molecular Genetics* 17(15): 2357-2369.

Wang, Y., K. Smith, B. C. Waldman, A. S. Waldman. 2011. Depletion of the bloom syndrome helicase stimulates homology-dependent repair at double-strand breaks in human chromosomes. *DNA Repair* 10: 416-426.

Wu, D., A. R. Flannery, H. Cai, E. Ko, K. Cao. 2014. Nuclear localization signal deletion mutants of lamin A and progerin reveal insights into lamin A processing and emerin targeting. *Nucleus* 5(1): 66-74.